

7-11-2013

# DEVELOPMENT OF SURFACE BASED PLATFORMS FOR BIOMOLECULAR RECOGNITION AND PROTEASE ASSAYS

Jose Cornejo

Follow this and additional works at: [https://digitalrepository.unm.edu/cbe\\_etds](https://digitalrepository.unm.edu/cbe_etds)

---

## Recommended Citation

Cornejo, Jose. "DEVELOPMENT OF SURFACE BASED PLATFORMS FOR BIOMOLECULAR RECOGNITION AND PROTEASE ASSAYS." (2013). [https://digitalrepository.unm.edu/cbe\\_etds/41](https://digitalrepository.unm.edu/cbe_etds/41)

This Thesis is brought to you for free and open access by the Engineering ETDs at UNM Digital Repository. It has been accepted for inclusion in Chemical and Biological Engineering ETDs by an authorized administrator of UNM Digital Repository. For more information, please contact [disc@unm.edu](mailto:disc@unm.edu).

Jose Alberto Cornejo

*Candidate*

---

Chemical And Nuclear Engineering

*Department*

---

This thesis is approved, and it is acceptable in quality and form for publication:

*Approved by the Thesis Committee:*

Dr. Steven Graves, Chairperson

---

Dr. James Freyer

---

Dr. Andrew Shreve

---

---

---

---

---

---

---

---

---

---

**DEVELOPMENT OF SURFACE BASED PLATFORMS FOR  
BIOMOLECULAR RECOGNITION AND PROTEASE ASSAYS**

By

**JOSE A. CORNEJO**

**B.S., CHEMICAL ENGINEERING, 2009  
M.S., CHEMICAL ENGINEERING, 2013**

THESIS

Submitted in Partial Fulfillment of the  
Requirements for the Degree of

**Master of Science  
Chemical Engineering**

The University of New Mexico  
Albuquerque, New Mexico

**May 2013**

**Dedication**

*This thesis is dedicated to my loving wife Vicki for her for all her  
love, support, and for her infinite patience in the process of  
building this thesis. And to my parents and sisters for all their love  
and encouraging words*

## ACKNOWLEDGEMENTS

I would like to express my appreciation to the members of my committee of studies: Dr. Steven Graves (advisor and chair), Dr. James Freyer, and Dr. Andrew Shreve. Thank you for your constant support and instruction. Your unconditional mentorship and efforts to push me towards excellence in research practices will resonate in my future endeavors. Thank you Dr. Graves for all of your support, for pushing towards excellence at all times, you have played a crucial part in my professional development. I would like to extend my appreciation to Dr. Gabriel Lopez for his mentorship, support and for introducing me to biomedical engineering research. This has truly been a positive learning experience that has made me a better researcher. Thank you all for your professional guidance.

This study was in part funded by the National Science Foundation's Partnership for Research and Education in Materials (PREM), the National Institutes of Health's Initiative for Maximizing Student Development (IMSD), and the National Flow Cytometry Resource.

I would like to acknowledge everyone that has helped me through this process. Dr. Linnea Ista, Dr. Menake Piyasena, Dr. Nesia Zurek, Carl Brown III, Kevin Cushing, Andrew Goumas, Matthew Rush, Travis Woods, Jingshu Zhu, and Michael Zubelewicz thank you for your thoughtful inputs and relevant discussions directly related to this study.

Additional thanks to Dr. Margaret Werner-Washburne for all her encouraging words that have helped me grow professionally and personally. To Dr. Menake Piyasena for all his training, immediate supervision, and for requiring my best at all times. Travis

Woods for all his uncompensated time instructing me in instrumentation usage, all his technical training, and his willingness to help with any technical issues in the laboratory. To all the wonderful people that make up the Center for Biomedical Engineering for making this a positive, fun, and very productive environment.

# **Development of Surface Based Platforms for Biomolecular Recognition and Protease Assays**

**By**

**Jose A. Cornejo**

**B.S., Chemical Engineering, University of New Mexico, 2009**  
**M.S., Chemical Engineering, University of New Mexico, 2013**

## **ABSTRACT**

The discovery of analytical tools for biomolecular recognition in the area of diagnostics is a research trend rich in innovative methods. Some of the main drivers found in this area are the constant need for low cost devices and biosensors, simplicity in design and operation, and time efficiency. In this thesis we present novel approaches for the development of protease activity assays. Our focus of study is the protease assay development process on two types of characterized platforms: microspheres and self-assembled monolayers (SAMs) on flat surfaces. The surface preparation and conjugation process with biological components of interest is presented along with surface plasmon resonance (SPR) and flow cytometry results.

These platforms were engineered in order to develop assays for bacterial toxin activity. Bacterial toxins are comprised in part of proteases, which selectively cleave peptides bonds in proteins. In this thesis we present, protease assays from our main focus of studies, the *Clostridium botulinum* Neurotoxin type A Light Chain (BoNTA/LC) metalloprotease. Supplementary studies include assays performed involving the *Bacillus anthracis* Lethal factor metalloprotease. In the work described we have prepared active

recombinant protease substrates in our laboratory, capable of binding with the surfaces of study. In addition, we present methods to on how to address non-specific binding issues inherited by the nature of these assays. Commercially available recombinant proteases have been utilized throughout these studies. These studies present novel methods for BoNT protease detection based on previous microsphere-based assays. Our biomimetic detection platforms show promise for further understanding BoNTs toxicity, the biological pathways of BoNTs substrates, and possible contributions to the discovery of protease inhibitors.

# Table of Contents

<b>List of Figures</b> .....	X
<b>Chapter 1: Introduction</b> .....	1
1.1 Current Protease Studies in Flow Cytometry .....	1
1.2 Background Information on BoNT Proteases and their Substrates.....	1
1.3 Novel Approaches for Protease Activity Assays .....	2
References.....	4
<b>Chapter 2: Surface-based Protease Assays for SPR Analysis</b> .....	6
2.1. Introduction .....	6
2.1.1 Surface Plasmon Resonance Background Information .....	6
2.1.2 SPR Sensor Chips for Protease Detection Assays .....	8
2.2. Materials and Methods .....	10
2.2.1 SAMs Formation and Development of SPR Sensor Chips.....	10
2.2.2 Surface Characterization.....	11
2.2.3 Construction of Biotinylated Substrate SNAP-25 GFP Plasmids .....	11
2.2.4 Expression and Purification of SNAP-25 GFP Protease Substrate .....	11
2.2.5 Binding SNAP-25 GFP Substrate to SPR Sensor Chips.....	13
2.3. Results .....	14
2.3.1 Surface Characterization.....	14
2.3.2 Binding Assays Analysis .....	15
2.3.3 BoNTA/LC Protease Assay Analysis .....	17
2.3.4 Lethal Factor Protease Assay Analysis.....	20
2.3.5 Implementation of Protease Assays in Alternate SPR Instrument.....	21
2.4. Discussion and Conclusions.....	22
References.....	24

<b>Chapter 3: Packed Bed Microfluidic Devices for Protease Assays .....</b>	<b>25</b>
3.1. Introduction .....	25
3.1.1 Packed Bed Microfluidics in Biotechnology .....	25
3.1.2 Protease Assays Inside Packed Bed Microfluidic Devices.....	26
3.2. Materials and Methods .....	27
3.2.1 Fabrication of Microfluidic Channels .....	27
3.2.2. Preparation of Biosensing Particles .....	29
3.2.3. Microfluidic Channel Characterization .....	30
3.3. Results .....	31
3.3.1 Qualitative Protease Activity Experiments .....	31
3.3.2 Quantitative Protease Activity Experiments .....	33
3.4. Discussions and Conclusions .....	35
3.4.1 Fabrication of Packed Bed Microfluidic Channels .....	35
3.4.2 Protease Activity Assays .....	36
References .....	38
<b>4. Biomimetic Platforms for Protease Diagnostics .....</b>	<b>39</b>
4.1. Introduction .....	39
4.1.1 SNARE Proteins and their Role in Neurotransmitter Release.....	39
4.1.2 Supported Lipid Bilayers on Microspheres in Bioanalytical Applications ....	41
4.1.3 Biomimetic Protease Detection Platforms for Flow Cytometry.....	42
4.2. Materials and Methods .....	43
4.2.1. Surface Treatment of Silica Microspheres .....	43
4.2.2. Preparation of Supported Lipid Bilayers.....	44
4.2.3. Lipid Stability Analysis via Fluorimetry and Flow Cytometry.....	45
4.2.4 Biomolecular Assembly and Protease Assays for Flow Cytometry.....	46
4.3. Results .....	46
4.3.1 Lipid Stability Analysis .....	46
4.3.2 Biomolecular Assembly and Protease Assays for Flow Cytometry .....	48
4.4. Discussion and Conclusions .....	53
4.4.1 Supported Lipid Stability.....	53

4.4.2 Biomimetic Platforms for Protease Activity Assays .....	53
References .....	55
<b>5. Conclusions and Recommendations for Future Work.....</b>	<b>57</b>
5.1 Surface-based Protease Assays for Surface Plasmon Resonance Analysis .....	57
5.1.1 Conclusions .....	57
5.1.2 Recommendations for Future Work .....	59
5.2 Packed-bed Microfluidic Devices for Protease Analysis .....	60
5.2.1 Conclusions .....	60
5.2.2 Recommendations for Future Work .....	61
5.3 Biomimetic Platforms for Protease Diagnostics .....	62
5.3.1 Conclusions .....	62
5.3.2 Recommendations for Future Work .....	64
References .....	65

## List of Figures

Figure 2-1. The Kretschmann SPR configuration .....	7
Figure 2-2. SPR sensor chip development.....	9
Figure 2-3. Surface characterization of SPR sensor chip by contact angle measurements	13
Figure 2-4. Components of a commercial SPR system .....	14
Figure 2-5. SPR sensorgram for surface protein immobilization .....	15
Figure 2-6. Hypothetical sensorgram for protease detection and activity assays .....	16
Figure 2-7. BoNTA/LC protease assay I .....	18
Figure 2-8. BoNTA/LC protease assay II.....	19
Figure 2-9. Lethal factor protease assay I.....	20
Figure 2-10. Lethal factor protease assay II.....	21
Figure 2-11. Lethal factor protease assay III .....	22
Figure 3-1. Microfabrication process and assembly steps for microchannel fabrication ..	28
Figure 3-2. Finished packed-bed microfluidic channel for protease activity detection.....	29
Figure 3-3. Protease substrate binding to streptavidin beads.....	30
Figure 3-4. Protease assay imaging .....	32
Figure 3-5. Photobleaching Control.....	32
Figure 3-6. Packing process of cleaved and uncleaved substrate bound to beads .....	33
Figure 3-7. Fluorimetric analysis of cleaved SNAP-25 GFP substrate .....	35
Figure 4-1. Representation of the neuromuscular junction and components of interest ...	40
Figure 4-2. Disulfide bond formation between cysteine residues from SNAP-25 and thiolated SLBs.....	43
Figure 4-3. Fluorescein-Lipid stability tests using flow cytometry .....	48
Figure 4-4. Flow cytometry tests for specificity of SNAP-25 attachment to thiolated SLBs.....	50
Figure 4-5. SNAP-25 GFP binding test comparison after 7 days of SLB formation .....	50
Figure 4-6. Reduction of 100% POPC SLBs using DTT .....	51
Figure 4-7. Reduction of 98% POPC and 2% PTE SLBs on beads using DTT .....	52
Figure 4-8. BoNTA/LC protease assay on PTE/POPC SLBs on beads .....	52
Figure 5-1. Recombinant SNARE protein with six terminal histidines binds to Ni-NTA functionalized SLBs on microspheres.....	64

# **Chapter 1**

## **Introduction**

### **1.1 Current Protease Studies in Flow Cytometry**

Flow cytometry is a technique capable of analyzing information in individual cells as well as in microspheres. This is why flow cytometry has been utilized extensively in the studies of microsphere as molecular carriers for the development of a wide variety of assays<sup>1,2</sup>. Furthermore, advances in flow cytometry feature multiplexible bead-based assays for high throughput screening and drug discovery<sup>3</sup>. As a result, flow cytometry has been utilized for the studies of multiplexible Botulinum neurotoxin (BoNT) protease assays and high throughput screening for drug targeting<sup>4,5</sup>. Adequate assays require proper bio-conjugation of microspheres for the analysis of substrate/protease interactions at their surfaces. Based on these studies, we have incorporated recombinant protein technologies, surface preparation, and protease assay development to our designs and applications of novel methodologies for BoNT protease activity detection.

### **1.2 Background Information on the BoNT Proteases and their Substrates**

Muscle contraction, a very important feature in humans, is the result of interactions between muscle cells and neurons. Major contributors for these interactions are the Soluble N-ethylmaleimide Sensitive Fusion Attachment Protein Receptors (SNAREs). These proteins are located inside neurons and act together in order to anchor synaptic vesicles with the neuron's outer membrane<sup>6</sup>. This anchoring effect enables the release of the neurotransmitter acetylcholine outside of the neuron and the subsequent binding to

acetylcholine receptors at the muscle cell's membrane. Along with subsequent reaction steps, these reaction pathways are in charge of assuring a normally functioning nervous system. Botulinum neurotoxins high toxicity is due to their ability to directly interfere with neurotransmitter release, thus causing muscle paralysis and death<sup>7</sup>. There are seven BoNT serotypes known to target SNARE proteins and specifically cleave them<sup>8</sup>. The SNARE protein complex is comprised of synaptobrevin, syntaxin and synaptosomal-associated protein 25 (SNAP-25), which is covered in this thesis.

### **1.3 Novel Approaches for Protease Activity Assays**

In chapter 2 we introduce the use of gold-coated surfaces containing self-assembled monolayers (SAMs) as surface plasmon resonance (SPR) biosensors. Due to the facility provided by SPR to perform protein adsorption on SAMs<sup>9</sup>, we present protease activity assays tailored for SPR analysis. BoNT proteases follow a single-substrate mechanism of enzymatic reaction<sup>10</sup>. Therefore, SPR allows one to differentiate in real time between BoNTA/LC substrate binding and catalytic events (substrate cleavage). Adequate protein adsorption methods are crucial for the success of these assays. As such, we have taken into account a significant amount of information from publications reporting proper recombinant protein expression and purification techniques. Substrate plasmids were based on Promega PinPoint biotinylation tag vectors due to their abundance and availability in our laboratory. This approach, coupled with avidin resin filtration matrices, is known to yield high levels of soluble biotinylated proteins<sup>11</sup>. Taking this technology into consideration along with previous binding studies<sup>12</sup>, we present fabricated biotinylated SPR sensor chips for the immobilization of streptavidin that allow the binding of succeeding biotinylated proteins.

In chapter 3 we explore the advantages of packed bed microfluidic channels for protease activity analysis. In them, we analyze sequestered streptavidin bearing microspheres to be coupled with our prepared biotinylated substrate proteins containing GFP markers. Packed beads in microchannels provide a high surface area to volume ratio, thus reducing analyte diffusion distances<sup>13</sup> and providing high sensitivity in the limits of protease detection. Here, we show how fluorescence-based protease assays are tailored for the use of fluorescence microscopy and fluorimetry.

In chapter 4 we present the utility of supported lipid bilayers on silica microspheres as biomimetic platforms for BoNT protease detection. It is suggested that membrane proteins interact with these biomimetic platforms while maintaining their functionality<sup>14,15</sup>. Therefore, our efforts have been focused on the design of supported lipid bilayers (SLBs) on microspheres capable of mimicking protein interactions with the neuron's plasma membrane. Taking into consideration the palmitoylation process, which will be explained in chapter 4, we have explored several types of lipids with moieties capable of forming selective bonds with thiol group from cysteines residues found in SNAP-25<sup>16</sup>. As a result, our studies also address ways of minimizing non-specific binding throughout the process development of protease assays using flow cytometry.

## References

1. Sklar, L. A., *Flow Cytometry for Biotechnology*. 2005.
2. Edwards, B. S.; Oprea, T.; Prossnitz, E. R.; Sklar, L. A., Flow cytometry for high-throughput, high-content screening. *Current Opinion in Chemical Biology* **2004**, *8* (4), 392-398.
3. Saunders, M. J.; Graves, S. W.; Sklar, L. A.; Oprea, T. I.; Edwards, B. S., High-Throughput Multiplex Flow Cytometry Screening for Botulinum Neurotoxin Type A Light Chain Protease Inhibitors. *Assay and Drug Development Technologies* **2010**, *8* (1), 37-46.
4. Edwards, B. S.; Zhu, J.; Chen, J.; Carter, M. B.; Thal, D. M.; Tesmer, J. J. G.; Graves, S. W.; Sklar, L. A., Cluster cytometry for high-capacity bioanalysis. *Cytometry Part A* **2012**, *81A* (5), 419-429.
5. Sudhof, T. C., THE SYNAPTIC VESICLE CYCLE - A CASCADE OF PROTEIN-PROTEIN INTERACTIONS. *Nature* **1995**, *375* (6533), 645-653.
6. Arnon, S. S.; Schechter, R.; Inglesby, T. V.; Henderson, D. A.; Bartlett, J. G.; Ascher, M. S.; Eitzen, E.; Fine, A. D.; Hauer, J.; Layton, M.; Lillibridge, S.; Osterholm, M. T.; O'Toole, T.; Parker, G.; Perl, T. M.; Russell, P. K.; Swerdlow, D. L.; Tonat, K.; Working Grp Civilian, B., Botulinum toxin as a biological weapon - Medical and public health management. *Jama-Journal of the American Medical Association* **2001**, *285* (8), 1059-1070.
7. Wortzman, M. S.; Pickett, A., The Science and Manufacturing Behind Botulinum Neurotoxin Type A-ABO in Clinical Use. *Aesthetic Surgery Journal* **2009**, *29* (6), S34-S42.
8. Schiavo, G.; Matteoli, M.; Montecucco, C., Neurotoxins affecting neuroexocytosis. *Physiological Reviews* **2000**, *80* (2), 717-766.
9. Mrksich, M.; Sigal, G. B.; Whitesides, G. M., SURFACE-PLASMON RESONANCE PERMITS IN-SITU MEASUREMENT OF PROTEIN ADSORPTION ON SELF-ASSEMBLED MONOLAYERS OF ALKANETHIOLATES ON GOLD. *Langmuir* **1995**, *11* (11), 4383-4385.
10. Saunders, M. Microsphere based protease assays and high throughput screening of bacterial toxin proteases. Dissertation, University of New Mexico, 2010.
11. Ashraf, S. S.; Benson, R. E.; Payne, E. S.; Halbleib, C. M.; Gron, H., A novel multi-affinity tag system to produce high levels of soluble and biotinylated proteins in *Escherichia coli*. *Protein Expression and Purification* **2004**, *33* (2), 238-245.

12. Morgan, H.; Taylor, D. M.; Dsilva, C., SURFACE-PLASMON RESONANCE STUDIES OF CHEMISORBED BIOTIN STREPTAVIDIN MULTILAYERS. *Thin Solid Films* **1992**, *209* (1), 122-126.
13. Piyasena, M. E.; Buranda, T.; Wu, Y.; Huang, J. M.; Sklar, L. A.; Lopez, G. P., Near-simultaneous and real-time detection of multiple analytes in affinity microcolumns. *Analytical Chemistry* **2004**, *76* (21), 6266-6273.
14. Chemburu, S.; Fenton, K.; Lopez, G. P.; Zeineldin, R., Biomimetic Silica Microspheres in Biosensing. *Molecules* **2010**, *15* (3), 1932-1957.
15. Diaz, A. J.; Albertorio, F.; Daniel, S.; Cremer, P. S., Double cushions preserve transmembrane protein mobility in supported bilayer systems. *Langmuir* **2008**, *24* (13), 6820-6826.
16. Daily, N. J.; Boswell, K. L.; James, D. J.; Martin, T. F. J., Novel Interactions of CAPS (Ca<sup>2+</sup>-dependent Activator Protein for Secretion) with the Three Neuronal SNARE Proteins Required for Vesicle Fusion. *Journal of Biological Chemistry* **2010**, *285* (46), 35320-35329.

## Chapter 2

### Surface-based Protease Assays for Surface Plasmon Resonance Analysis

#### 2.1 Introduction

##### 2.1.1 Surface Plasmon Resonance Background Information

Surface plasmon resonance (SPR) is a physical phenomenon that is originated by the reflection of incident laser light (this is the case of the SPR instruments presented in this work) upon a thin metal film. Surface plasmons are oscillations of free electrons, that when excited into resonance by applying such light source, the incident light is absorbed by the metal film triggering a low intensity reflection<sup>1</sup> (see figure 2-1). During this resonance event, and with the aid of a material with a high refractive index such as a prism, one can formulate a relationship between the dielectric constants of the metal film (e.g. gold-coated film) and the testing medium (e.g. proteins in buffer solution) to the angle of light incident onto the metal film. Such relationship is expressed by equation 2-1:

$$\sin(\Theta_R) = \sqrt{\frac{\epsilon_1 \epsilon_m}{(\epsilon_1 + \epsilon_m) \epsilon_2}} \quad \text{eq. 2-1}$$

Where  $\epsilon_1$  is the dielectric constant of the testing medium,  $\epsilon_2$  is the dielectric constant of the prism and  $\epsilon_m$  is that of the exposed sensor metal film. Our SPR instrumentation is designed following the Kretschmann configuration, where the light source is located on the glass side of the thin film, which is the opposite side of the metallic layer. As

molecules reach the metal surface the local index of refraction changes, thus shifting the resonance angle. This phenomenon makes SPR a high detection sensitivity method and a label-free technique for the immobilization of biomolecules.

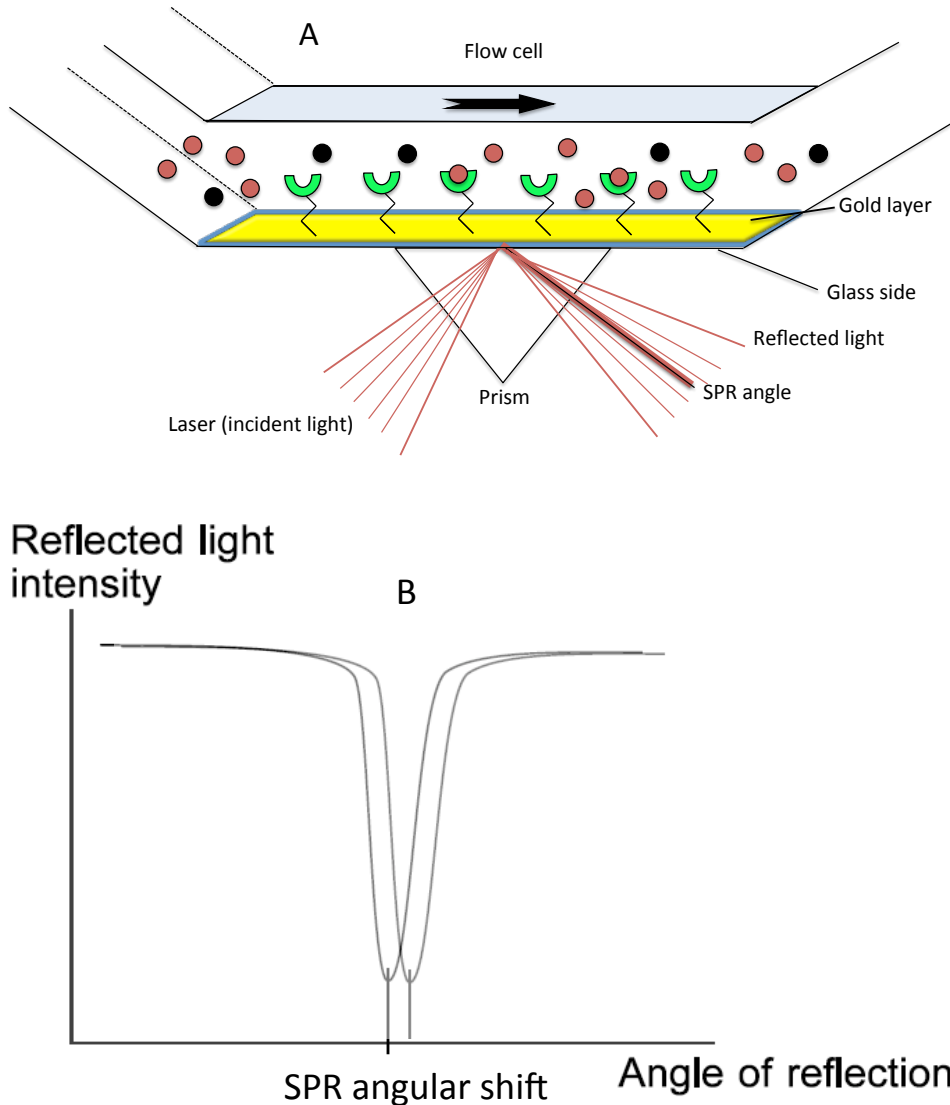


**Figure 2-1.** The Kretschmann SPR configuration. (A) The light source is located on the opposite side of the metallic layer, that is, the glass side. (B) A plasmon is an electron charge density wave at the metal film that is excited by the incident light due to its energy and angle of incidence. Absorption of energy occurs causing surface plasmons. This phenomenon is described by the decrease in reflected light intensity as a function of the angle of reflection (SPR angle is located at the minimum).

### 2.1.2 SPR Sensor Chips for Protease Detection Assays

SPR studies described in this work consist of gold-covered thin films because of the metal's small real refraction index and large imaginary refraction index for the wavelengths of optical excitation<sup>2</sup>. Because of these physical properties, gold is presented as a suitable candidate for biosensor nanotechnology and therefore, a suitable substrate for SPR studies. In addition, it is known that gold binds thiols with high affinity<sup>3</sup>, providing high SAM stability for several days if in contact with a liquid medium.

Functionalized thiols were used as the building backbones for all SPR chips. Their fabrication process consists of two steps. First, the surface of thin glass cover slips is modified by thermal vapor gold deposition. Second, self-assembled monolayers (SAMs) are formed on the surface of the gold-treated thin films by submersion in ethanol solutions containing biotin-functionalized thiols. We followed this methodology because it was crucial to alleviate biosensor costs. Protease assays on commercially available functionalized SPR biosensors specifically designed for biotinylated protein capturing present elevated costs due to surface regeneration issues. As a result, we present a less expensive alternative consisting of formed SAMs specifically designed for streptavidin immobilization and further interactions with biotinylated receptors. In addition, we had several components readily available in our laboratory for the fabrication of SAMs such as gold and a metal evaporator for gold deposition.

As mentioned in the previous section, SPR allows us to measure bound analyte on biosensors using a label-free type of detection, in real time. Therefore, we implemented the development of BoNT protease assay to this approach in order to monitor the molecular interactions between substrate and protease. The compounds of interest in our

SPR studies included proteases from Botulinum neurotoxins and anthrax lethal toxins. Such proteases interact with their respective substrates (host proteins) by cleaving them at specific sites<sup>4,5</sup>. The importance of this work lays on the increasing interest of the study of such proteases due to their role in natural disease<sup>6</sup>, their potential use in bioterrorism<sup>6</sup>, and therefore the exploration for approaches to recognize effective inhibitors. This chapter is devoted to the exploration of activity and detection assays related to these components. We hypothesized that given successful binding of streptavidin and SNAP-25 biotinylated substrate to a sensor chip, we could be able to monitor for specific activity of the BoNTA/LC protease and study important parameters such as reaction times and amount of mass bound or dissociated from the sensor surface at all times by using SPR.

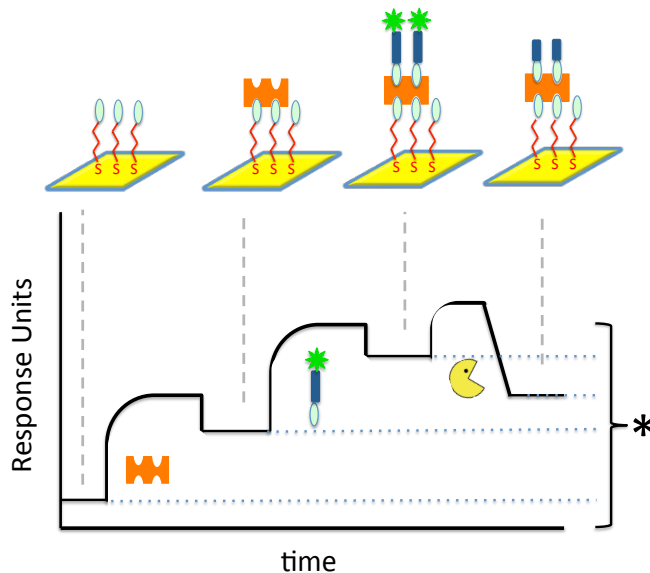


**Figure 2-2.** Hypothetical sensorgram for protease detection and activity assays. The first binding curve represents the binding of streptavidin to biotinylated SAMs at the SPR chip surface. The second binding curve corresponds to biotinylated protease substrate binding to the streptavidin-rich SPR chip. The third binding curve represents the initial binding of a protease to its specific substrate, and subsequent cleavage. \*The cleavage effect and any other binding events will be quantified by the calculation of amount of mass gained or lost at the surface of the SPR chip by monitoring the change in response units at the given reference points. Thus, a decrease in response units will be expected at the end of an experimental run.

## **2.2 Materials and Methods**

### **2.2.1 SAMs Formation and Development of SPR Sensor Chips**

SAMs were prepared as previously described<sup>7, 8</sup>. Microscope cover slips were prepared by immersing them in piranha solution (30% H<sub>2</sub>O<sub>2</sub> and 70% H<sub>2</sub>SO<sub>4</sub>). CAUTION: piranha solution reacts violently with most organic materials thus causing burns to the skin. It must be handled with extreme care in a certified safety hood with fully personal protective equipment. They were then rinsed with DI water and absolute grade ethanol and dried by a nitrogen stream prior to being placed in a vacuum chamber to begin the gold-coating process. The coating process was done by thermal evaporation deposition of 2nm of chromium and 50 nm of gold 99,999% in purity (Plasmaterials, Livermore, CA). For the formation of SAMs, the freshly gold-coated cover slips were submerged for a minimum of 16 hours in a solution containing 1 mM biotin-terminated tri-(ethylene glycol) undecanethiol (Asemblon, Seattle, WA) in ethanol (200 proof, Fisher Scientific, Waltham, MA). When ready for experimentation, the SAMs were rinsed with ethanol and dried under nitrogen.

### **2.2.2 Surface Characterization**

Once the biotin-terminated SAMs were formed, they were analyzed by surface wettability measurements. Contact angles from water drops on the SAMs were measured using a Ramé-Hart Model 100 goniometer (Succasunna, NJ). Drops were placed on three different regions randomly selected and an average of 3 angle measurements per drop was acquired. These measurements allowed us to measure the hydrophobicity of the

biotin-containing SAMs and to corroborate with previous wettability calculations on identical surfaces reported in the literature.

### **2.2.3 Construction of biotinylated substrate SNAP-25 GFP plasmids**

SNAP-25 GFP protease substrate plasmids were based on the Promega PinPoint technology<sup>9</sup>. These vectors featured a biotinylation tag at the N terminus and enhanced green fluorescence protein (EGFP) cloned at the C terminus. The SNAP-25 GFP expression plasmid was produced by restriction digest of the Xa sub-plasmid and ligation of a SNAP-25 PCR product that was obtained from a SNAP-25 clone plasmid. Transformation of these plasmid ligations was performed in competent BL21 (DE3) pLys S *E. coli* by following the miniprep method (Qiagen).

### **2.2.4 Expression and Purification of SNAP-25 GFP Protease Substrate**

Transformation of BL21 (DE3) pLys S *E. coli* calcium competent cells was performed as previously described<sup>10</sup>. Briefly, transformed bacterial cells with SNAP-25 GFP plasmid were grown overnight at 37°C in 3 mL of TB media with the addition of 50 µg/mL of carbenicillin and 34 µg/mL chloramphenicol in order to enable antibiotic resistance. They were then transferred to 250 mL of TB containing 50 µg/mL of carbenicillin, 34 µg/mL chloramphenicol, and 40 µM biotin. Incubation followed until the cultures reached an optical density at wavelength 600 nm between 0.6 and 0.8. Cultures were then induced with 100 µM Isopropyl β-D-1-thiogalactopyranoside (IPTG, Life Technologies) and grown at 30°C overnight. Cells were spun down at 4000 rpm for

30 min on a centrifuge at 4°C, suspended in lysis buffer (50 mM Tris-HCl, 1mM ethylenediaminetetraacetic acid (EDTA), 100 mM NaCl, pH 8.3), and frozen at -20°C.

Once ready for protein purification, frozen cells were thawed on ice, sonicated for 10 min, and centrifuged at 4°C at 14000 rpm for 30 min. The soluble fraction was loaded onto a Fast protein liquid chromatography (FPLC, GE Healthcare) containing 5mL of Softlink streptavidin resin (Promega). The product was eluted using 1mM dithiothreitol (DTT), 5 mM biotin in phosphate buffer saline (PBS). The fractions were centrifuged in an Amicon Ultra-15 30,000 molecular weight cutoff filter for 10 min at 4,000 rpm at 4°C in order to remove free biotin and thus, reduce non-specific binding affecting the protease assays. The purified protein was then dialyzed for 3 rounds against 3 L of 50 mM HEPES, 100 mM NaCl, pH 7.4 for 4 hours each round. Final protein was determined using A280 spectroscopic measurements given that the extinction coefficient for biotinylated SNAP-25 GFP was calculated to be 28,740 cm<sup>-1</sup>M<sup>-1</sup>.

### **2.2.5 Binding SNAP-25 GFP Substrate to SPR Sensor Chips**

Gold-coated sensor chips containing thiolated SAMs were docked to surface plasmon resonance instrument (Biacore X100, GE Healthcare) which was primed by running buffer consisting of 50 mM HEPES, 100 mM NaCl, 1 mg/mL BSA, 0.025% Tween 20, pH 7.4 through the instrument's flow cell. Once a stable baseline was achieved (see Fig?), streptavidin at concentrations ranging from 0.1 to 1 μM was injected at a flow rate of 10 μL/min for 10 minutes. This was followed by the injection of biotinylated SNAP-25 GFP substrate at concentrations ranging from 100 nM to 500 nM.

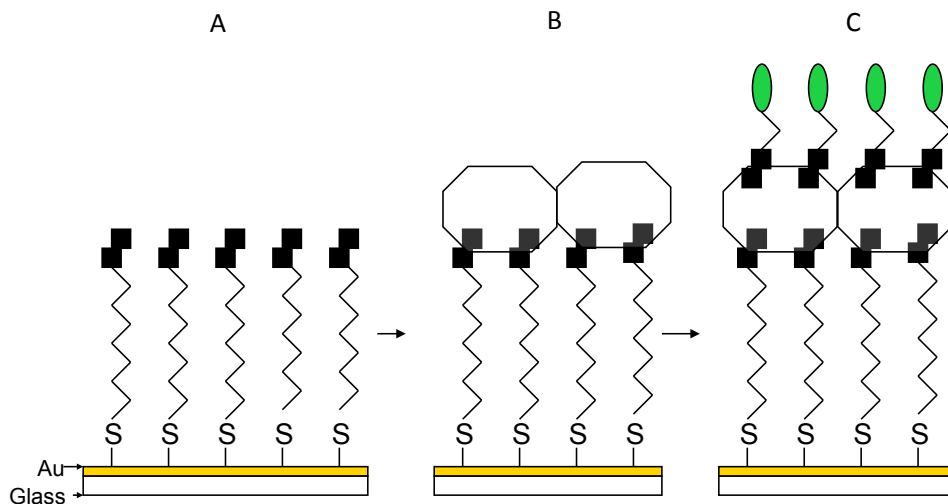


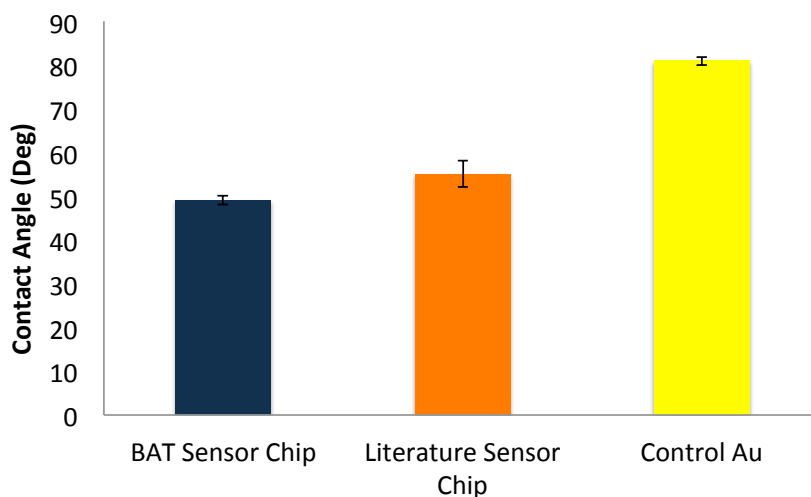
**Figure 2-3.** SPR sensor chip development. A) Self-assembled monolayers consisting of biotinylated alkyl thiols (BATs) attached to a gold-covered coverslip after being submerged in ethanol solution containing 1 mM BAT. Thus, the surface was made compatible to be used as a sensor chip for surface plasmon resonance instruments. B) Once introduced to the SPR instrument, streptavidin was injected at different concentrations in order to specifically bind to the biotin receptors at the SAMs by using its first pair of binding pockets. C) Upon streptavidin immobilization, a biotinylated substrate protein is introduced to bind to the second binding pairs from each streptavidin molecule.

Recombinant Botulinum neurotoxins type A and type F light chain proteases and Anthrax Lethal Factor protease were obtained from List Biological Laboratories (Campbell, CA). Each protease vial was resuspended in protease buffer to a concentration of 0.1 mg/mL.

## 2.3 Results

### 2.3.1 Surface Characterization

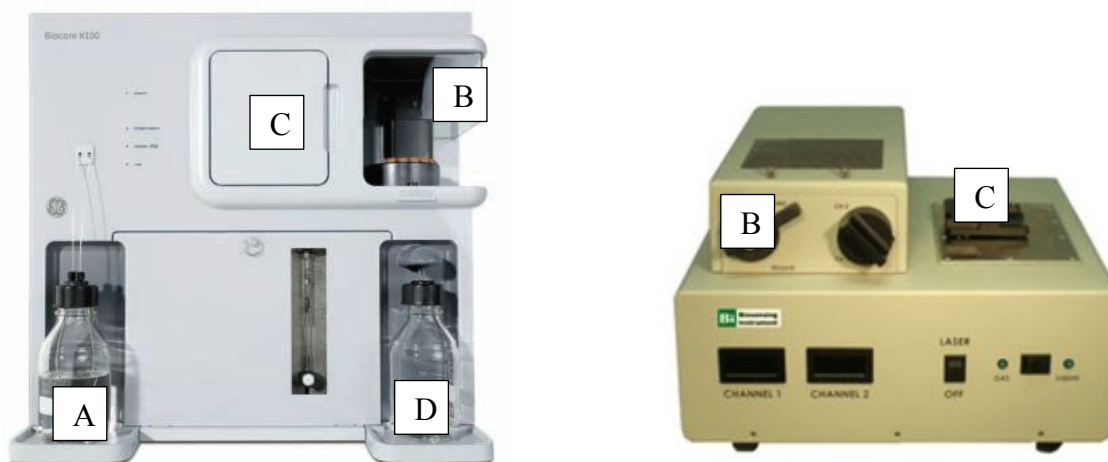
Surface analysis of the SAMs was performed by contact angle measurements by determining the degree of hydrophobicity of the surface in question. Biotin-terminated SAMs presented a water contact angle of  $49 \pm 1^\circ$ . Previous wettability studies on an identically prepared surface reported a water contact angle of  $55 \pm 3^\circ$ .<sup>8</sup> As expected the bare gold surface presented a more hydrophobic environment. This was used as a reference point to verify that modification of gold substrates by using monolayers of biotin-terminated tri-(ethylene glycol) undecanethiol creates a more hydrophilic surface.



**Figure 2-4.** Surface characterization of SPR sensor chip by contact angle measurements. Blue: Contact angle of biotinylated SAM used as SPR sensor chips in protease assays. Orange: Contact angle from identical biotinylated alkyl thiol SAM reported in the literature.<sup>8</sup> Yellow: Contact angle of bare gold-covered surface.

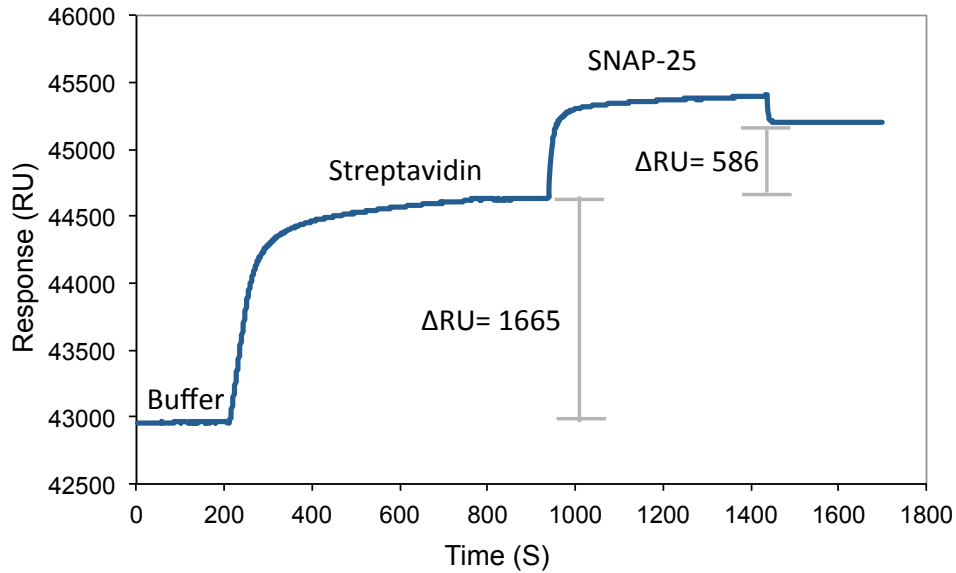
### 2.3.2 Binding Assays Analysis

Figure 2-4 presents the components of a commercial SPR instrument. Buffer present in reservoir (A) and the injecting sample rack (B) are mixed at the flow cell platform (C) right before molecular recognition by SPR.



**Figure 2-5.** Components of a commercial SPR system. GE Biacore (left) and Biosensing Instrument (right). (A) Buffer reservoir. (not pictured in BI system) (B) Sample collection deck. In the case of BI system, each sample is injected with a Hamilton syringe at the sample port. (C) Optics region. Buffer and samples arrive to this platform through the instrument's tubing system at laminar flow. There, a flow cell transports them to the SAMs-rich gold surface. In the BI SPR system, buffer reservoir is not pictures (D) Waste reservoir.

At the start of every run, buffer was first introduced to the Biacore X-100 SPR system as it traveled through the instrument's tubing system at laminar flow and reached the interrogation region composed of the SAMs-covered gold surface enclosed by the instrument's flow cell. Figure 2-6 shows a binding assay incorporating streptavidin and SNAP-25 GFP starting with a steady baseline from the introduction of running buffer to the system and finishing with the partial dissociation of SNAP-25 GFP from the surface of the SPR chip.



**Figure 2-6.** SPR sensorgram for surface protein immobilization. This sensorgram indicates the amount of streptavidin and biotinylated SNAP-25 GFP bound to the sensor chip as a function of time. One response unit (RU) is equivalent to 0.0001° of angular shift in the refractive index.

Figure 2-6 features a binding curve between biotinylated SNAP-25 and streptavidin containing three different phases: the association phase (rise), the equilibrium phase, and the dissociation phase (drop). These processes can be represented by first-order bimolecular reaction expressed as follows:



where A represents streptavidin bound to the SPR chip, B represents SNAP-25 as sample solution introduced into the flow cell of the system. The term  $k_a$  is the association rate constant and  $k_d$  is the dissociation rate constant. Thus, the reaction rate can be monitored by the SPR response (R) signal at time t:

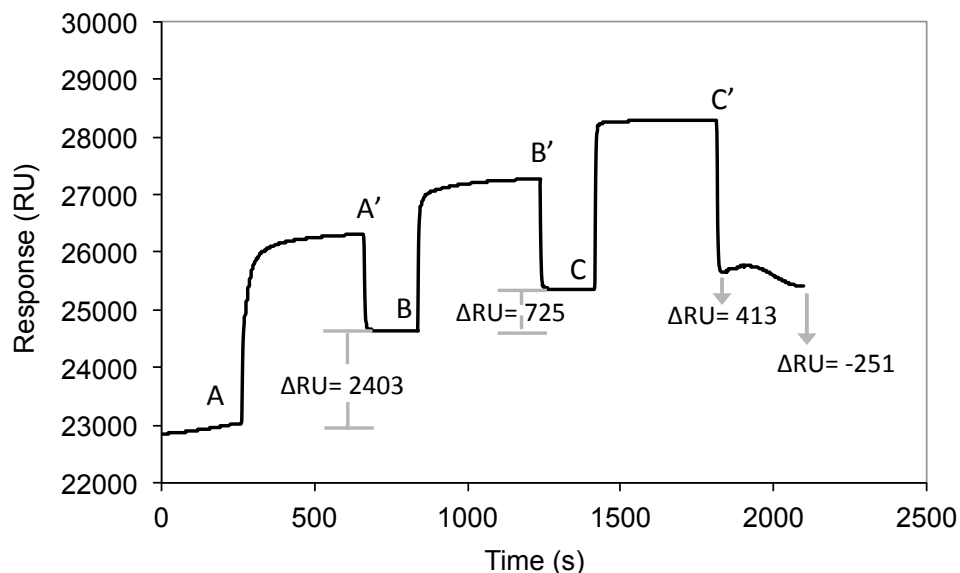
$$\frac{dR}{dt} = k_a C(R_{\max} - R) - k_d R \quad \text{eq. 2-3}$$

where R is the SPR signal at time t, C is the concentration of SNAP-25 and  $R_{\max}$  is the maximum signal response of SNAP-25 molecules bound to the sensor chip. Therefore, we were able to quantify the amount of molecules that remain bound to the sensor surface and the amount of molecules that dissociate from the surface sensor. Likewise, the dissociation phase can be described by the following equation:

$$\frac{dR}{dt} = -k_d R \quad \text{eq. 2-4}$$

### 2.3.3 BoNTA/LC Protease Assay Analysis

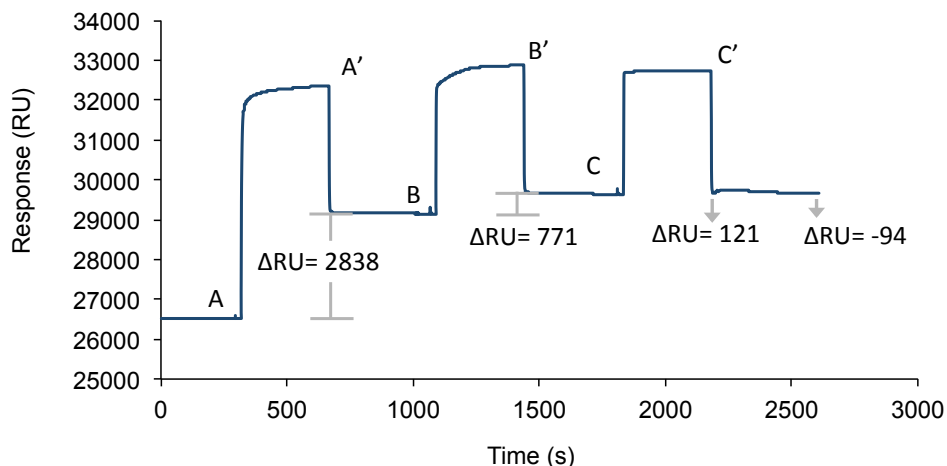
After repeated successful binding assays such as the one presented in figure 2-6, we proceeded to test this biosensing platform for BoNTA/LC protease activity. After injection of the biological components previously described, BoNTA/LC protease was injected at concentrations not exceeding 20 nM. All components were introduced at equal volumes. It is important to state that the SPR computer program calculates the time of sample injection, which is directly proportional to the volume of the sample that is being analyzed. Therefore all samples were injected at equal times except for buffer washing steps of smaller volumes containing a given amount of BSA in order to reduce non-specific binding. Protease assays were performed within 10 days of opening our commercial recombinant BoNTA/LC vial in order to prevent denaturation.



**Figure 2-7.** BoNTA/LC protease assay I. (A-A') Injection of streptavidin. (B-B') Injection of SNAP-25 GFP. (C-C') BoNTA/LC protease injection. Observed decrease in response near the end of the sensorgram is associated with presumed protease activity.

From these SPR sensorgrams, one can easily differentiate between the time it takes for the protease to bind with its substrate and the time involved with the proteolytic activity leading to cleavage of the substrate. Further experimentation shows a second sensorgram (figure 2-8) showing both the substrate-binding step and the proteolytic step triggering less pronounced changes in SPR response compared to those in figure 2-7. While all components and concentrations were handled in a similar way as in the first experiment, this run was performed at a later time. At the end of the experimental run we observed a decrease in response of 251 RUs compared to the point right after the end of the protease injection (approximately at the 1800-second mark). However, the observed decrease in response did not reach the level corresponding to the SNAP25 substrate, thus

showing no signs of cleavage (proteolytic activity). One explanation for lack of cleavage in this instance can be attributed to the possibility of the protease undergoing protein denaturation due to its high sensitivity to temperature changes and time after its suspension in buffer.



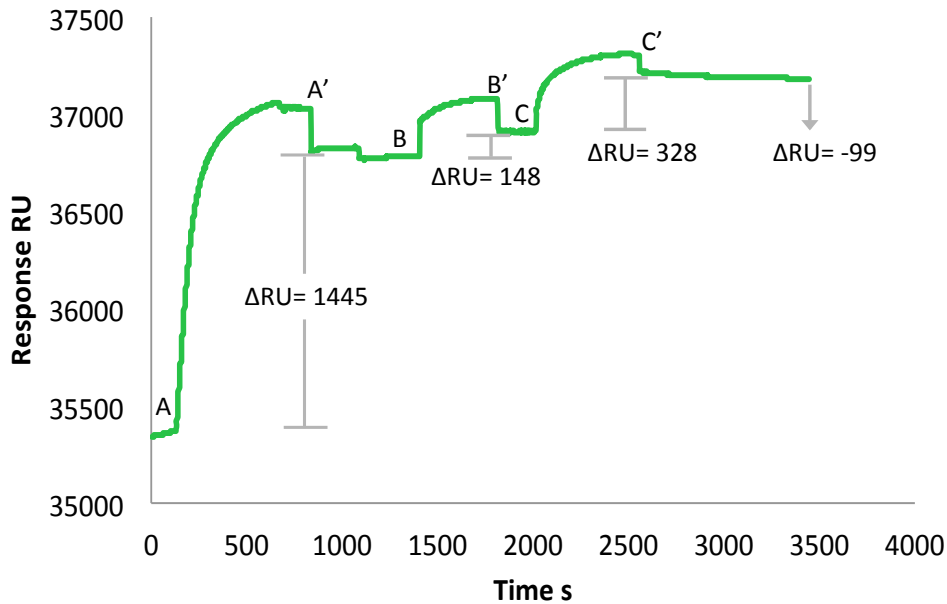
**Figure 2-8.** BoNTA/LC protease assay II. (A-A') Streptavidin injection. (B-B') SNAP-25 GFP injection. (C-C') injection BoNTA/LC protease sample. We monitored for protease cleavage by comparing the completed BoNTA/LC protease injection time point (association step) to response signal at the last recorded time point. Protease response shows near- complete dissociation after the substrate-binding step. Response signal from proteolytic step showed a decrease of 94 RU.

Figure 2-8 presents the same scenario presented in figure 2-7. While we can observe a decrease in response after protease injection, there is no cleavage associated with this decrease because of the response ending above the recorded level after SNAP-25 substrate injection.

### 2.3.4 Lethal Factor Protease Assay Analysis

A similar protease assay was performed for the detection of the anthrax toxin lethal factor protease. We obtained the recombinant protease substrate for following the same

expression and purification protocols described in section 2.2. This biotinylated substrate contained the active cleavage regions for lethal factor protease and it was designated as LF-15 GFP. Similar results were obtained showing unsuccessful protease cleavage by the lethal factor protease although a decrease of 99 RUs was recorded.



**Figure 2-9.** Lethal factor protease assay I. (A-A') Injection of streptavidin. (B-B') Injection of LF-15 GFP substrate. (C-C') Injection of lethal factor protease. Protease substrate-binding step gave a response signal of 328 RU while the proteolytic step presented a decrease of 99 RU.

When an identical lethal factor protease assay was performed (figure 2-10) a more pronounced decrease is appreciated, which reaches the level prior to SNAP-25 injection. Because of this, the detection of protease cleavage is still unclear. In addition, the response signal following streptavidin injection seem is very similar to that following protease injection. At first, they appear to be bound to the sensor surface after dissociation response signals but then, further dissociation occurs. This leads to further discussion on the specificity of protease cleavage, which will be covered in chapter 5.

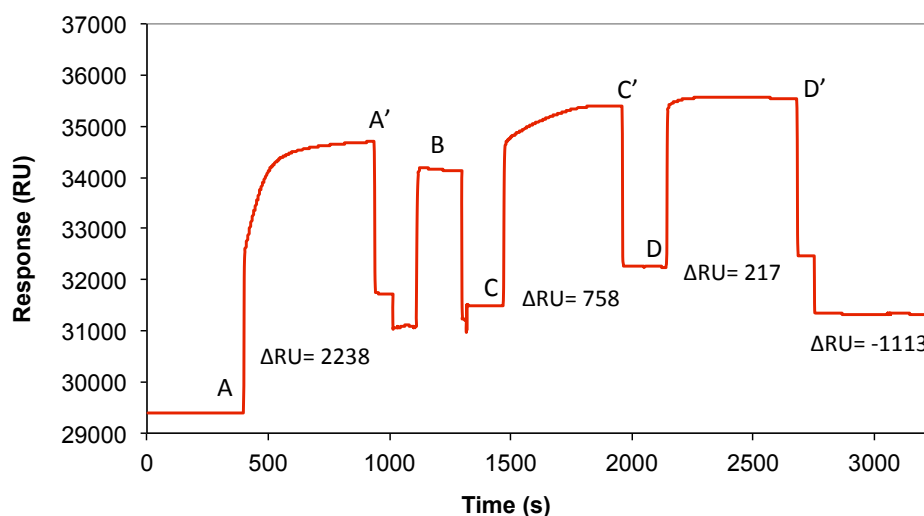


**Figure 2-10.** Lethal factor protease assay II. (A-A') Injection of streptavidin. (B) Block injection of 1 mg/mL BSA. (C-C') Injection of LF-15 GFP substrate. (D-D') Injection of lethal factor protease. Apparent cleavage is seen by lethal factor proteolytic activity. Further analysis suggests cleaving effect is non-specific due to similar decrease in response signal found after streptavidin binding as well as in after protease binding.

### 2.3.5 Implementation of Protease Assays in Alternate SPR Instrument

Our facilities possess two SPR instruments: a GE Biacore X100 and a BI SPR. In order to verify the reproducibility of these protease detection assays, we performed a lethal factor protease detection assay by using both instruments. Results from the BI SPR are shown in figure 2-11. Response signals of the binding steps corresponding to streptavidin and LF-15 GFP are in good agreement with previous results using the Biacore X100. Lethal factor protease shows minimal response during its substrate-binding time.

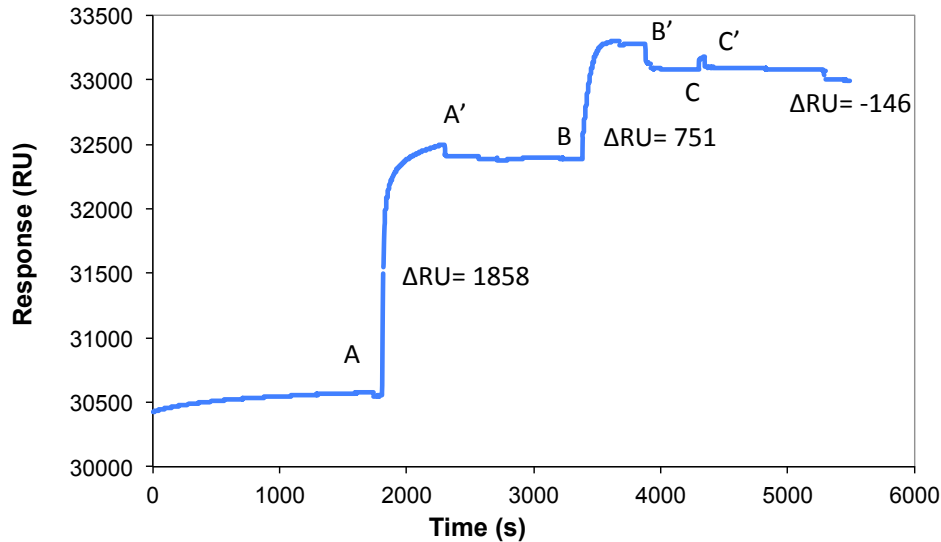


**Figure 2-11.** Lethal factor protease assay III performed in Biosensing Instrument SPR system. (A-A') Streptavidin injection. (B-B') LF-15 GFP injection. (C-C') Lethal Factor protease injection. In order to corroborate the reproducibility of the results from the Biacore SPR instrument, we opted to perform protease assays by using a second SPR instrumentation (BI SPR).

## 2.4 Discussion and Conclusions

We have successfully purified protease substrate proteins comprising of three domains: the biotinylation sequence, the full-length substrate containing the BoNT-LC cleaving region, and a EGFP domain. While the latter one is often utilized as the fluorescence reporter domain for a variety of binding assays<sup>11</sup>, in this case, this region contributed to the amount of mass to be cleaved upon protease activity.

We have successfully developed SPR sensor chips for streptavidin attachment. These chips were surface-treated by chemisorption of biotinylated alkyl thiols on gold-covered glass films, forming monolayers. Furthermore, these sensor chips have been effectively tested by performing binding assays via biotin-streptavidin-biotin building blocks. Such experiments provided useful information on the binding capacities of the SPR sensor

chips by calculating the amount of mass bound to their surface by measuring the angle of maximum plasmon resonance, represented by response units (RU). We have reported such binding activity by using two types of SPR instruments: Biacore X100 and BI SPR. Both systems present similar binding response curves up to the point of injection of the protease substrate. We conclude that both the Biacore X100 SPR system and the BI-2000 SPR system are suitable devices for our studies. This is supported by binding curves generated by these instruments showing similar streptavidin and SNAP-25 adsorption profiles. However the Biacore X100 SPR system is more time efficient at reaching equilibrium before and after every injection, thus reducing background noise and providing stability throughout the experiments. In chapter 5 we will further discuss and propose methods to improve these protease activity assays.

## References

1. Raether, H., SURFACE-PLASMONS ON SMOOTH AND ROUGH SURFACES AND ON GRATINGS. *Springer Tracts in Modern Physics* **1988**, *111*, 1-133.
2. Love, J. C.; Estroff, L. A.; Kriebel, J. K.; Nuzzo, R. G.; Whitesides, G. M., Self-assembled monolayers of thiolates on metals as a form of nanotechnology. *Chemical Reviews* **2005**, *105* (4), 1103-1169.
3. Nuzzo, R. G.; Allara, D. L., ADSORPTION OF BIFUNCTIONAL ORGANIC DISULFIDES ON GOLD SURFACES. *Journal of the American Chemical Society* **1983**, *105* (13), 4481-4483.
4. Rossetto, O.; Schiavo, G.; Montecucco, C.; Poulain, B.; Deloye, F.; Lozzi, L.; Shone, C. C., SNARE MOTIF AND NEUROTOXINS. *Nature* **1994**, *372* (6505), 415-416.
5. Vitale, G.; Pellizzari, R.; Recchi, C.; Napolitani, G.; Mock, M.; Montecucco, C., Anthrax lethal factor cleaves the N-terminus of MAPKKs and induces tyrosine/threonine phosphorylation of MAPKs in cultured macrophages. *Biochem. Biophys. Res. Commun.* **1998**, *248* (3), 706-711.
6. Bigalke, H.; Rummel, A., Medical aspects of toxin weapons. *Toxicology* **2005**, *214* (3), 210-220.
7. Nelson, K. E.; Gamble, L.; Jung, L. S.; Boeckl, M. S.; Naeemi, E.; Golledge, S. L.; Sasaki, T.; Castner, D. G.; Campbell, C. T.; Stayton, P. S., Surface characterization of mixed self-assembled monolayers designed for streptavidin immobilization. *Langmuir* **2001**, *17* (9), 2807-2816.
8. Perez-Luna, V. H.; O'Brien, M. J.; Opperman, K. A.; Hampton, P. D.; Lopez, G. P.; Klumb, L. A.; Stayton, P. S., Molecular recognition between genetically engineered streptavidin and surface-bound biotin. *Journal of the American Chemical Society* **1999**, *121* (27), 6469-6478.
9. Saunders, M. J.; Kim, H.; Woods, T. A.; Nolan, J. P.; Sklar, L. A.; Edwards, B. S.; Graves, S. W., Microsphere-based protease assays and screening application for lethal ZXF factor and factor Xa. *Cytometry Part A* **2006**, *69A* (5), 342-352.
10. Saunders, M. J.; Graves, S. W.; Sklar, L. A.; Oprea, T. I.; Edwards, B. S., High-Throughput Multiplex Flow Cytometry Screening for Botulinum Neurotoxin Type A Light Chain Protease Inhibitors. *Assay and Drug Development Technologies* **2010**, *8* (1), 37-46.
11. Zimmer, M., Green fluorescent protein (GFP): Applications, structure, and related photophysical behavior. *Chemical Reviews* **2002**, *102* (3), 759-781.

## **Chapter 3**

### **Packed-bed Microfluidic Devices for Protease Analysis**

#### **3.1 Introduction**

##### **3.1.1 Packed Bed Microfluidics in Biotechnology**

In this chapter, we describe a simple method of protease detection via fluorescence-based techniques on microspheres sequestered inside of packed bed microfluidic channels. Microfluidic devices have significantly contributed to the area of biomolecular analysis<sup>1</sup>, and continue to present new technologies<sup>2</sup>. In general, these systems are capable of performing at microliter to submicroliter volumetric regimes, therefore providing a viable alternative for the field of diagnostics in critical regions of the world where water treatment is a major concern. The design of such devices allow for fluid samples to be delivered and analyzed at laminar flow regimes, which allows one to address simple molecular diffusion constrains inherited by solution-based assays. The implementation of microspheres coupled with the development of packed bed regions inside the microchannels provides a surface area of analysis capable of molecular detection while keeping the overall cost for device fabrication low. Given the limitations observed when using gold chips bearing SAMs as SPR-based sensors, we turned our focus to the elaboration of these new platforms for protease assays development while simplifying the biomolecular detection process. Our objective in this section was to fabricate robust packed bed microfluidic devices capable of housing microspheres and biomolecular components used in protease detection. We introduced this method for the

first time to ongoing efforts of BoNTs protease analysis in for disease prevention. This was inspired by previous successful reports on quantitative and qualitative real-time studies in a broad range of applications such as bioaffinity assays, multianalyte detection,<sup>3</sup> and immobilization of metabolically active cells.<sup>4</sup>

The sensing methods described in this chapter are conformed by streptavidin-bearing polystyrene microspheres utilized in order to immobilize the biotinylated substrate SNAP-25 GFP that whose purification process was described in chapter 2. The importance of these studies is determined by the ability to effectively detect protease activity at the surface of the beads within the microchannel, as well as by the detection of protease cleavage of the substrate upon protease injection. We utilized fluorescence microscopy techniques incorporating the appropriate optics arrangement for GFP excitation and emission. The binding assays presented in this work are ultimately directed to explore loss of fluorescence detection techniques recognizing the cleaving effect by BoNTA/LC protease on its substrate therefore releasing the cleaved GFP-bound region away from the point of detection.

### **3.1.2 Protease Assays Inside Packed Bed Microfluidic Devices**

After the successful fabrication of these devices and with the additional information acquired from reports on microsphere-based BoNT protease assays<sup>5</sup>, we hypothesized that under laminar flow conditions, these protease-substrate interactions could be effectively detected by utilizing packed microspheres as sensing surfaces. Hence, it was expected that, with the aid of fluorescence microscopy, one could monitor the enzymatic reaction time by using imaging techniques. For example, this method provides feasibility

at recording images of packed beads with the SNAP-25 GFP substrate complex attached to their surfaces and compare that with subsequent images that present the loss of fluorescence due to protease cleavage over time. In addition, given the microchannel design presented in this study, we were able to detect loss of fluorescence at the surface of the entrapped microspheres and to quantify the amount of substrate cleaved by the protease by collecting the cleaved GFP-bound substrate region at the microchannel's outlet.

## **3.2 Materials and Methods**

### **3.2.1 Fabrication of Microfluidic Channels**

Microfluidic devices were fabricated using standard photolithographic and soft lithographic techniques.<sup>6</sup> In order to hold the beads in place, PDMS-based dams were incorporated to the fabrication design. Test grade N-type silicon wafers (WaferNet, San Jose, CA) were treated and developed into master molds for microchannel patterns. First, they were cleaned with piranha solution for 1 hour, rinsed with DI water and ethanol, and dried by a stream of N<sub>2</sub>. In order to create the dam at each channel, we applied two types of negative photoresists onto the silicon wafers and followed the manufacturer's processing guidelines. (See <http://microchem.com> for further information). Photoresist SU-8 2010 (MicroChem, Newton, MA) was used to spin-coat a layer of 10 μm in thickness. Second, a piece of Scotch tape of 0.8 to 1 mm wide was placed across the wafer. Third, SU-8 2075 (MicroChem, Newton, MA) was used to form a thicker layer of 75 μm. Upon soft baking, the tape was removed thus also removing the thicker photoresist layer underneath the tape. The microchannel-patterned mask was obtained

from CAD/Art Services, Bandon, OR. Once it was properly aligned with the photoresist-coated wafer, the sample was exposed to UV radiation.

The elastomeric polymer PDMS was used to form the microchannels as it cross-linked on the master mold. The time necessary to obtain a fully polymerized material was directly proportional to the temperature of sample incubation. Incubation temperatures varied from room temperature to 40° C. Then, cross-linked PDMS material was carefully removed from the master mold. The prepared PDMS channels were irreversibly sealed on to glass slides using an Ar plasma cleaner. This resulted in microfluidic channels 250  $\mu\text{m}$  in width, 2.5 cm in length, and 10  $\mu\text{m}$  in height at the dam, and 85  $\mu\text{m}$  in height elsewhere.

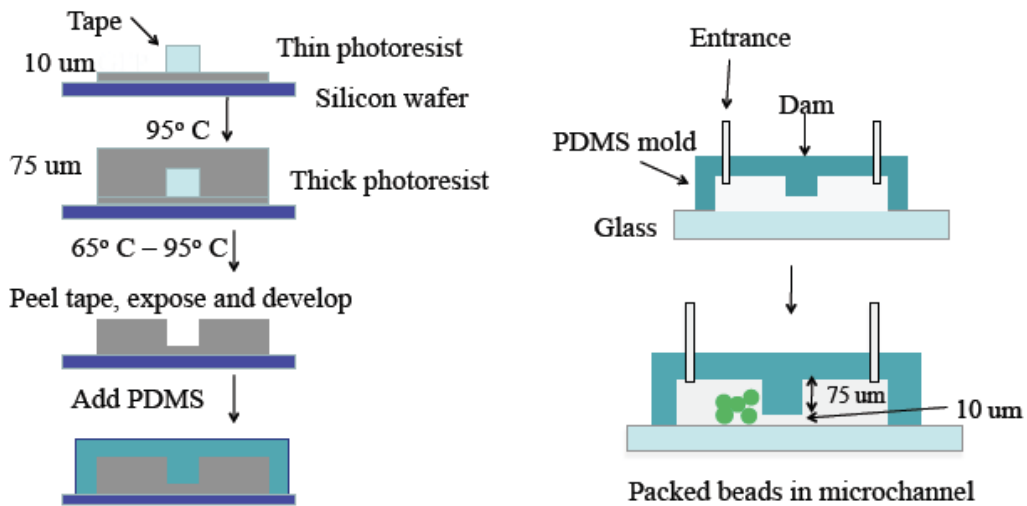


**Figure 3-1.** Microfabrication process and assembly steps for microchannel fabrication. Channel patterns including narrowing (dam) in the middle of the channel were developed by applying standard photolithography techniques on silicon wafers. Small dams were created for the packing of streptavidin coated-microspheres incubated with SNAP-25 GFP prior to microchannel packing. Once the device was finalized, channel dimensions consisted of 45 mm in length, 250  $\mu\text{m}$  in width, and 80  $\mu\text{m}$  in height. Height at the narrowing region (dam) is 10  $\mu\text{m}$ .

Finally, silicone tubes (Cole-Parmer, Vernon Hills, IL) of approximately 1 mm in inner diameter were cut at the same length and sealed into small perforations made on the PDMS channels to be used as inlets and outlets, see Figure 3-2.

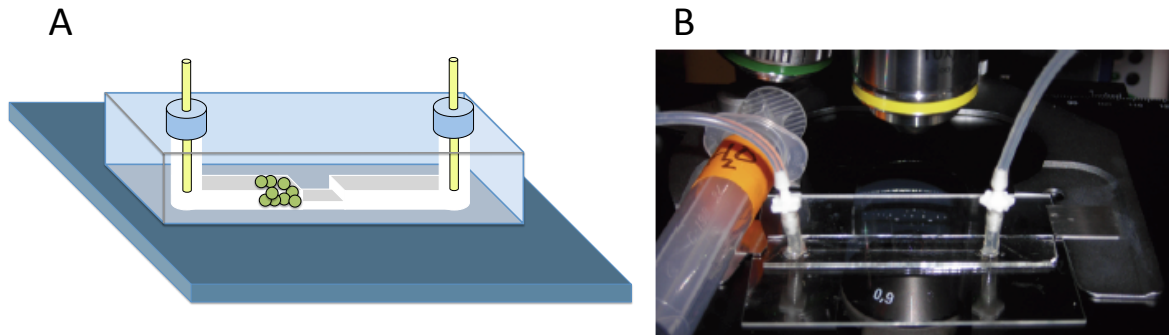


**Figure 3-2.** Finished packed-bed microfluidic channel for protease activity detection. (A) The device consists of a PDMS support sealed to a glass slide and additional PDMS and silicon tubing fittings. (B) Photograph of a single channel microfluidic device ready for analysis. Inlet (left) was connected to a plastic syringe containing loading buffer and pushed with the aid of a syringe pump. The outlet (right) was directed to a waste container.

### 3.2.2 Preparation of Biosensing Particles

22  $\mu\text{m}$  Streptavidin-coated polystyrene microspheres were obtained from Spherotec, Inc. The beads were washed 3 times with DI water and their concentration was of  $6.02 \times 10^6$  particles/ml, calculated with a Coulter Counter. The beads were resuspended in protease buffer (50 mM HEPES, 100 mM NaCl, 1mg/ml BSA, 0.025% (v/v) Tween 20, pH 7.4) in Eppendorf tubes. Subsequently, biotinylated substrate SNAP-25 GFP was added to the mixing Eppendorf tubes at different concentrations. The samples were incubated for 1 hr. in order to allow the biotinylated substrate to bind to the streptavidin-coated microspheres.

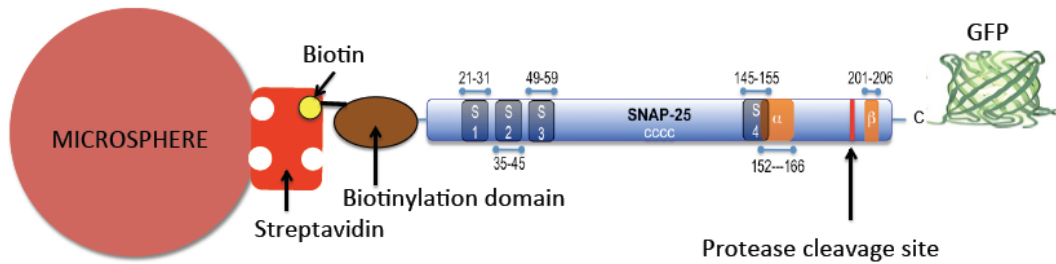


**Figure 3-3.** Protease substrate binding to streptavidin beads. Commercial streptavidin polystyrene beads were used for the attachment of biotinylated SNAP-25 GFP protease substrate in fluorescence-based assays.

### 3.2.3 Packing of Beads in Microchannels and Protease Injection

The device was attached to a syringe mounted on a Nexus 3000 syringe pump (Chemyx, Stafford, TX) in order to inject buffer or samples at a determined flow rate. Protease buffer was introduced to the microchannels in order to wet the walls and achieve a stable flow rate. Then, aliquots of 5  $\mu\text{L}$  of the microspheres were introduced to the channels with a pipette tip. The channels were packed by a layer of microspheres of at least 1 mm in length. Protease buffer flow was redirected to the channels so that they were kept wet. Upon flow stabilization, 10  $\mu\text{L}$  of 10nM to 30 nM light chain protease was injected to the device by using a 10  $\mu\text{L}$  Hamilton syringe and partially perforating the inlet silicone tubing. The interactions between the protease and the substrate loaded on the beads were monitored using a Zeiss Axio Imager A2 (**Carl Zeiss Microscopy**, Thornwood, NY) fluorescence microscope as the fluorescence signal of the GFP-covered beads changed upon cleavage of the substrate. Fluorescence experiments were performed using a blue light as the excitation source for GFP and a 520 nm band pass filter (Thorlabs, Newton, NJ) for emission detection. Such interactions were recorded over time by photo and video, using a CCD camera (Andor Technology, Belfast, UK).

A second set of experiments consisted of preparing two different bead samples. Sample 1 contained the beads incubated with the substrate as previously described. The second sample consisted of mixing the already prepared SNAP-25 GFP coated microspheres as in sample 1 with the addition of the BoNTA/LC directly to the Eppendorf tubes and incubated for 30 minutes. Then, sample 1 was introduced and packed in the microchannel. After achieving a significant amount of beads trapped at the dam, we introduced sample 2 which contained already cleaved substrates bound to the beads. Then, we compared the two different bead populations (uncleaved vs. cleaved substrate) by using the CCD camera's imaging capabilities. This was done in order to test the limits of detection of protease-substrate interactions happening inside the microchannels and those occurring inside a mixing tube prior to loading them inside the microchannels.

### **3.3 Results**

#### **3.3.1 Qualitative Protease Activity Experiments**

Two different qualitative experiments were performed in order to detect the protease activity of BoNTA/LC. The first one consisted in packing the prepared microspheres containing SNAP-25 GFP at the microchannel's dam and then injecting the BoNTA/LC protease. After injection, we monitored changes of fluorescence at the packed bed region with pictures at 10-minute intervals. The most significant change in fluorescence was observed after one hour of protease injection. Possible photobleaching issues were addressed by performing the same packing process in the absence of the protease and monitoring fluorescence changes over the same period of time. According to

the pictures from figure 3-5, fluorescence emitted from the beads remained constant as time progressed.

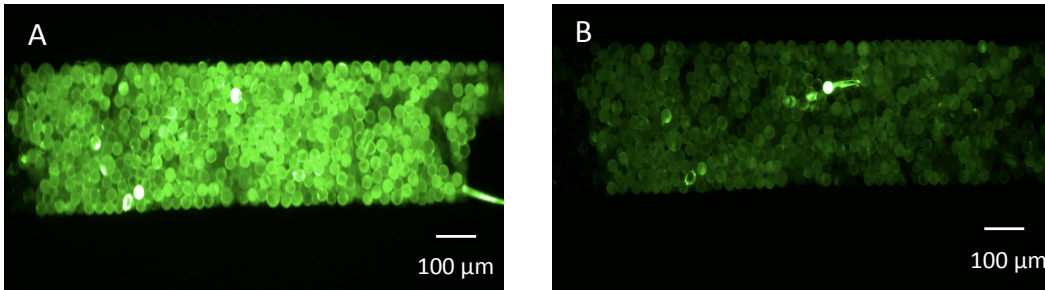


**Figure 3-4.** Protease assay imaging A) False color image of packed streptavidin beads bound to SNAP-25 GFP. 1 hour mixing was done prior to loading the device with beads. B) Decrease in GFP fluorescence intensity due to BoNTA/LC protease addition. The image was taken 1 hour after introducing the protease to the channel via Hamilton Syringe injection.

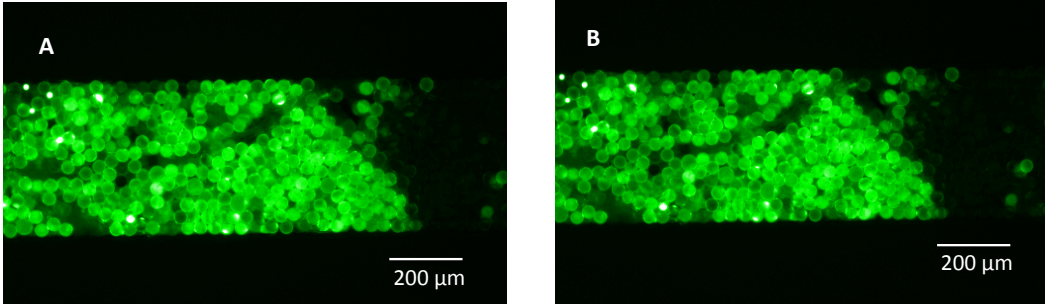


**Figure 3-5.** Photobleaching control. Packed streptavidin beads bound to SNAP-25 GFP were imaged in the absence of the protease at a constant flow rate. Fluorescence intensity from the beads was monitored for 1 hour.

Our second experimental procedure was driven by the need to compare the protease effect when mixed with the substrate-bound microspheres in mixing tubes with the effect when the components are mixed inside the microchannels. Therefore, we prepared two different samples containing the beads conjugated with the SNAP-25 GFP substrate complex after 1 hour of incubation. While the first sample was left unmodified, we added

the BoNTA/LC protease to the second sample for 30 additional minutes of incubation. The samples were introduced as described in figure 3-5. We observed that while the mixing times in both scenarios, protease molecular diffusion was faster when mixing occurred in mixing micro centrifuge tubes than when inside the microchannels.

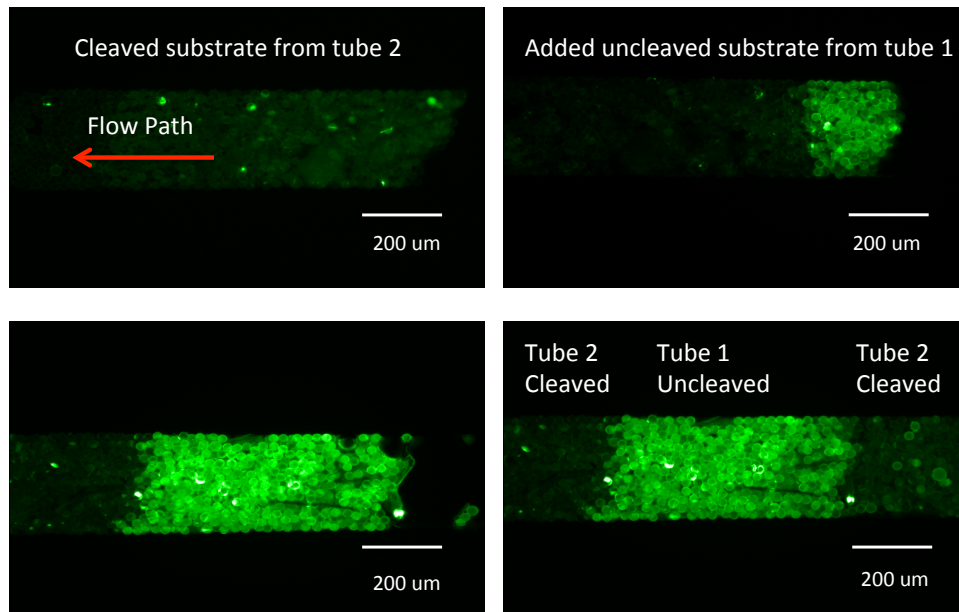


**Figure 3-6.** Packing process of cleaved and uncleaved substrate bound to beads. This comparison analysis was done in order to find the limitations of the device in protease assay performance. Tube 1: Mixed 22  $\mu\text{m}$  Streptavidin polystyrene beads with 500 nM biotin-SNAP25GFP for 1 hour Tube 2: Mixed 22  $\mu\text{m}$  Streptavidin polystyrene beads with 500 nM biotin-SNAP25GFP for 1 hour, then added 10 nM BoNTA/LC protease and mixed for 30 minutes.

### 3.3.2 Quantitative Protease Activity Experiments

It was also of importance to corroborate the qualitative studies by quantitatively determining the protease activity. Thus, we calculated the fluorescence decrease as a result of the protease acting upon the SNAP-25 GFP substrate complex by monitoring the amount of cleaved fluorescent mass at the device's outlet. By using a fluorimeter that is equipped with high sensitivity capabilities we intended to decrease the time of protease

recognition (it took 45 minutes to 1 hour to observe fluorescence decrease due to cleavage by using fluorescence microscopy). According to our protease assay design, the substrate region that was cleaved due to the BoNTA/LC protease was expected to detach from the microspheres and freely travel in flowing buffer towards the device's outlet. Thus, samples were collected from a reservoir connected to the outlet and examined by using a PTI QuantaMaster 30 Spectrofluorimeter (Photon Technology International, Birmingham, NJ). Thus, this allowed us to build a correlation between such fluorescence gain indicating the presence of cleaved GFP-bound substrate released to the collecting reservoir and the amount of fluorescence lost at the surface of the packed beads. The curve corresponding to 30 minutes after injection presents a higher peak than that corresponding to 10 minutes after injection. This was another proof of slow diffusion rates in which the longer the protease was allowed to be in contact with the beads, the higher the substrate cleavage was observed. The curve corresponding to buffer flow without protease also exhibited a peak at the GFP's emission peak of 507 nm. This can be explained by the presence of unbound SNAP-25 GFP molecules introduced along with the conjugated beads that mixed with the flowing buffer and were eventually carried away from the dam.

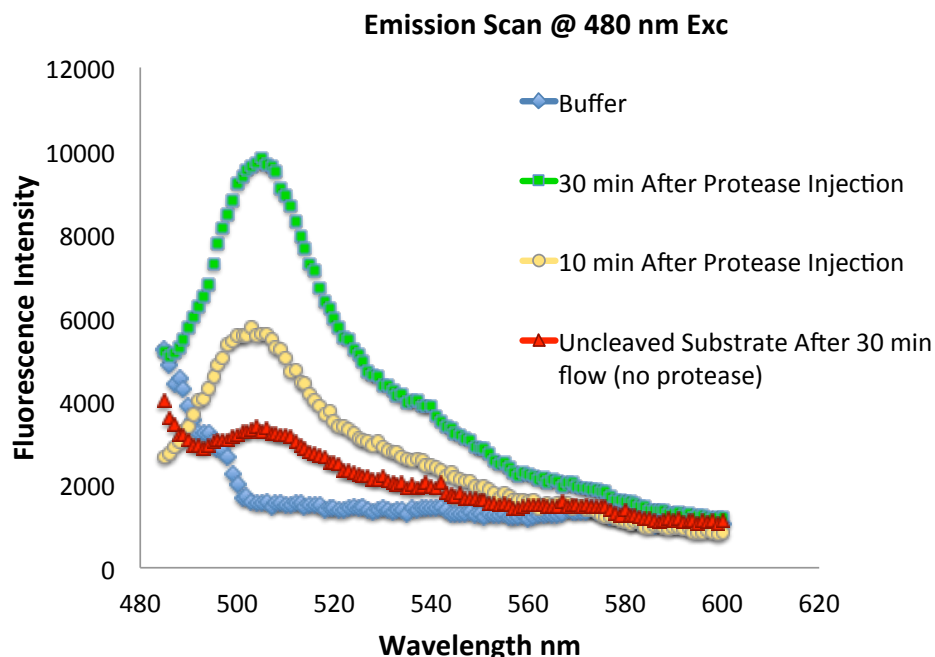


**Figure 3-7.** Fluorimetric analysis of cleaved SNAP-25 GFP substrate. Samples were collected in a reservoir after they exited the microfluidic device. All samples were diluted with buffer to reach 500  $\mu$ L for proper analysis using fluorimeter cuvettes via emission wavelength scanning. Blue: Buffer (50mM HEPES, 100 mM NaCl) used prior to injection into microfluidic device. Red: Flowing buffer collected after 30 minutes of flow through packed microspheres covered by SNAP-25 GFP. Yellow: Collection of cleaved GFP-bound substrate after 10 minutes of BoNTA/LC exposure. Green: Collection of cleaved GFP-bound substrate after 30 minutes of BoNTA/LC exposure.

### 3.4 Discussion and Conclusions

#### 3.4.1 Fabrication of Packed Bed Microfluidic Channels

We have been able to successfully fabricate packed bed microchannel devices capable of effectively sequestering bio-conjugated microspheres of diameter sizes above 10  $\mu$ m. These devices have therefore allowed us to design, test, and study BoNTA/LC protease-substrate interactions. Furthermore, the usefulness of these devices are not limited to these biological components but rather, they present a potential bioanalytical tool for a great variety of applications.<sup>4, 7</sup> We have demonstrated that our devices

fabricated in our laboratory can be successfully utilized in those areas. In addition, the devices fabricated in our laboratory were capable of sustaining increasing flow rates that reached 80  $\mu\text{L}/\text{min}$ , which was sufficient for the regimes delineated by our studies (i.e. 1-2  $\mu\text{L}/\text{min}$  in order to speed up protease diffusion). Finally, we have accomplished to design a simple method for biomolecular detection. Other important features of this approach also include portability, low consumption of analyte volume, and low cost in process fabrication.

### **3.4.2 Protease Activity Assays**

We have been able to monitor BoNTA/LC proteolytic activity by using qualitatively methods involving monitoring fluorescence changes with the aid fluorescence microscopy and imaging techniques. We were able to find a correlation between these findings and those from our designed quantitative methods utilizing fluorimetric techniques. Fluorescence decrease at the surface of the packed microspheres was noticeable after 1 hour of protease injection; which was done by taking photographs every 5 minutes under constant flowing buffer conditions (see figure 3-4). In contrast, from our quantitative experiments (see figure 3-7), we were able to observe that after 10 minutes upon protease release, fluorescence from cleaved SNAP-25 GFP molecules were already present at the end of the device's microchannel. Some of the disadvantages that we encountered involved transport limitations in the fluid flow of samples. Back pressure was originated due to the expansion of the PDMS-based microfluidic walls. This was an issue that was triggered by the microsphere conglomeration at the channel's dam. Also, we observed PDMS shards created at the dam region and at both ends due to the punching effect done to build the channels' inlets and outlets. These issues triggered

limited device functionality for our desired protease assays. The observed slow reaction times as shown in figure 3-4 can be attributed to these limitations. This lead to device reproducibility issues which triggered a variation in the fluid flow rate, in spite of setting our syringe pump at a constant flow rate throughout the experimentation process. Diffusion limitations may also be attributed to the dimensions of the microchannels, whose volume comprising of the inlet to the interrogation region was approximately 0.3  $\mu\text{L}$ .

## References

1. Quake, S. R.; Scherer, A., From micro- to nanofabrication with soft materials. *Science* **2000**, *290* (5496), 1536-1540.
2. Ingber, D. E.; Whitesides, G. M., Lab on a Chip: United States of America. *Lab on a Chip* **2012**, *12* (12), 2089-2090.
3. Buranda, T.; Huang, J. M.; Perez-Luna, V. H.; Schreyer, B.; Sklar, L. A.; Lopez, G. P., Biomolecular recognition on well-characterized beads packed in microfluidic channels. *Analytical Chemistry* **2002**, *74* (5), 1149-+.
4. Flemming, J. H.; Baca, H. K.; Werner-Washburne, M.; Brozik, S. M.; Lopez, G. P., A packed microcolumn approach to a cell-based biosensor. *Sensors and Actuators B-Chemical* **2006**, *113* (1), 376-381.
5. Saunders, M. J.; Graves, S. W.; Sklar, L. A.; Oprea, T. I.; Edwards, B. S., High-Throughput Multiplex Flow Cytometry Screening for Botulinum Neurotoxin Type A Light Chain Protease Inhibitors. *Assay and Drug Development Technologies* **2010**, *8* (1), 37-46.
6. Duffy, D. C.; McDonald, J. C.; Schueller, O. J. A.; Whitesides, G. M., Rapid prototyping of microfluidic systems in poly(dimethylsiloxane). *Analytical Chemistry* **1998**, *70* (23), 4974-4984.
7. Piyasena, M. E.; Buranda, T.; Wu, Y.; Huang, J. M.; Sklar, L. A.; Lopez, G. P., Near-simultaneous and real-time detection of multiple analytes in affinity microcolumns. *Analytical Chemistry* **2004**, *76* (21), 6266-6273.

## **Chapter 4**

### **Biomimetic Platforms for Protease Diagnostics**

#### **4.1 Introduction**

##### **4.1.1 SNARE Proteins and their Role in Neurotransmitter Release**

In this chapter we study protease sensing methods while emphasizing the biological role of the SNARE protein complex in neurotransmitter release and hence, in neuron-to-muscle cell communication<sup>1,2</sup>. This information is crucial for the process of better understanding the interactions between the BoNT/LC proteases and their substrate counterparts. Studies suggest that the binding capability of SNAP-25 to cell membranes is thanks to its four-cysteine residues<sup>3</sup>. SNAP-25 associates with membranes by undergoing the process of palmitoylation<sup>4</sup>. This natural process has been a key element for the design biomimetic systems capable of being utilized in the development of protease detection assays. Hence, here we provide information on how to recreate SNAP-25 GFP palmitoylation given proposed biomimetic systems consisting of supported lipid bilayers (SLBs) formed on silica microspheres. Our results will lead to clearer pathways for the implementation of the other two SNARE complex proteins: syntaxin, and vesicle-associated membrane protein (VAMP) in protease assays by incorporating multiplex flow cytometry in our studies. This will allow us to conjugate three types of microspheres varying in size with the three different SNARE proteins and therefore simultaneously analyze the different bead populations. These efforts will be important contributing

factors with ongoing research towards understanding the role of SNARE protein complex in synaptic vesicle fusion<sup>5, 6, 7</sup>, and in disease triggered by foreign proteolytic activity<sup>8, 9</sup>.

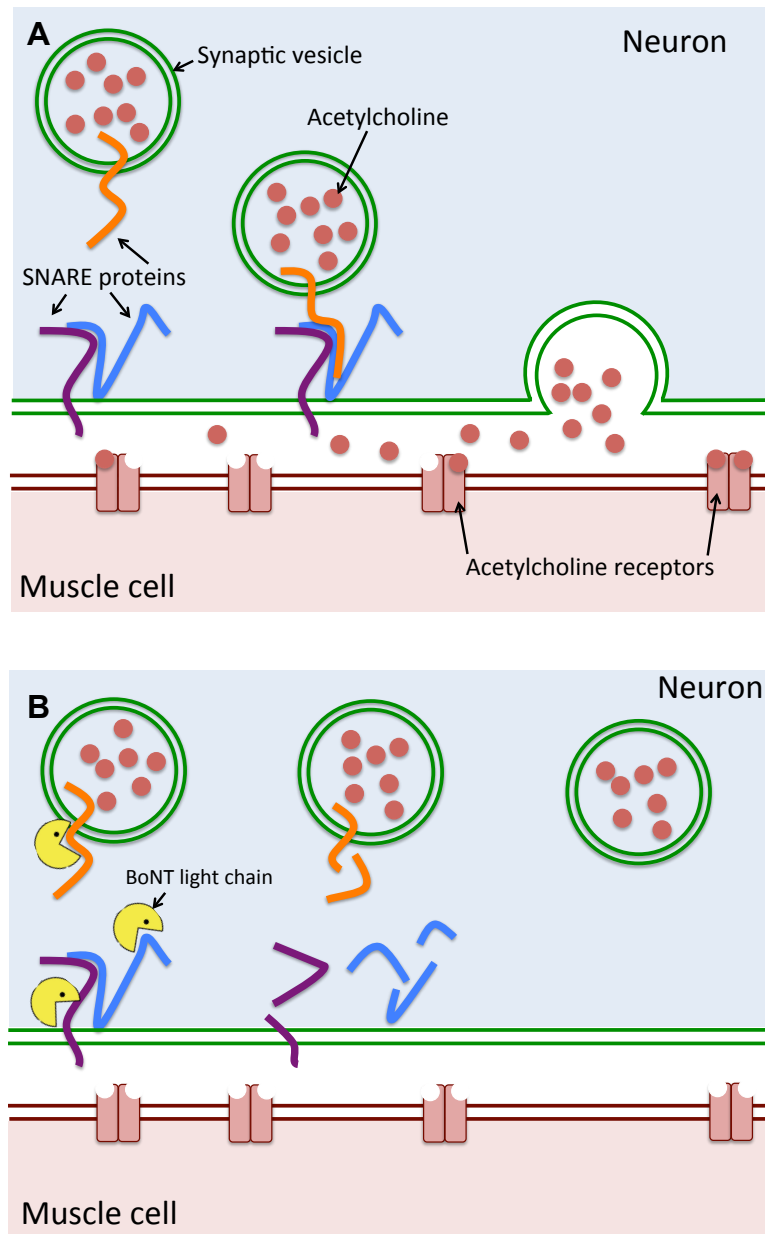


**Figure 4-1.** Representation of the neuromuscular junction and components of interest. A) Role of SNARE proteins in neurotransmitter Acetyl Choline release. SNARE proteins: Syntaxin, Synaptobrevin, Synaptosomal-associated protein 25kDa (SNAP-25) mediate docking and fusion between the synaptic vesicles and the plasma membrane of the neuron, ultimately allowing muscle stimulation. These proteins are affected when the host contracts botulism disease. B) BoNT light chain proteases selectively cleave the SNARE proteins thus preventing acetylcholine release and causing paralysis and death.

#### **4.1.2 Supported Lipid Bilayers on Microspheres in Bioanalytical Applications**

Supported lipid bilayers (SLBs) are formed by the interactions of two layers of amphiphilic phospholipids, where their hydrophobic tails are oriented inwards facing one another, and their hydrophilic heads are oriented outwards. Due to this spontaneous configuration,<sup>10</sup> and their ability to mimic the structure of biological membranes, SLBs on microspheres have been used extensively in the area of biosensing.<sup>11</sup> In addition, a wide variety of membrane proteins can be incorporated to SLB-microsphere structures through different anchoring methods. Because of this, and from the information gathered in section 4.1.1, we introduced the SLB-bead configuration into our protease sensing studies. The immobilization of SNARE proteins on functionalized lipid bilayers creates an attractive bioanalytical method for the development of protease assays. Furthermore, the incorporation of microspheres to the analytical carrying platform allows one to utilize flow cytometry as an analytical tool for fluorescence-based biomolecular detection. Flow cytometry is a powerful tool that measures fluorescence intensity bound to every microsphere, and neglects free fluorescence from solution surrounding the microspheres. In conventional flow cytometry, microspheres are focused via hydrodynamic focusing in such a way that they travel down in the flow cell in single file. Thus, this technique becomes advantageous for purposes of performing real-time protease assays, an important feature that has been emphasized throughout this thesis. In addition, one disadvantage of SAMs and streptavidin-coated polystyrene beads as model surfaces is that they are essentially static. This characteristic differs from that of biological membranes, which are fluid and rearrange dynamically.

### 4.1.3 Biomimetic Protease Detection Platforms for Flow Cytometry

As stated in chapter 1, the natural attachment of SNAP-25 *in vivo* by reactions occurring between the protein's cysteine residues and the synaptic lipid vesicles inside the neuron. This process is referred to as palmitoylation.<sup>12</sup> Located in the peripheral nervous system, this process plays a central part in the initiation of release of the neurotransmitter acetylcholine to the exterior of the neuron, which subsequently allows acetylcholine molecules to bind to their specific receptors bound to the plasma membrane of muscle cells. The main function of this type of neuron-to-muscle cell chemical communication is to allow normal contraction of skeletal and smooth muscles.

As a result, our protease assay developmental process will be enhanced and will provide a pathway for the design of biomimetic protease detection platforms. In order to mimic natural conditions and obtain relevant information from such conditions we constructed supported lipid bilayers on porous silica microspheres. We hypothesized that by utilizing supported lipid bilayers consisting of a small molar fraction of thiol-containing functionalized lipids we would be capable of specifically building disulfide bridges between the substrate protein complex (i.e. natural tetra cysteine motif found in SNAP-25) and the existing thiols from the lipo-microsphere structure. Furthermore, we would be able to demonstrate the enhancement of our protease assay development due to our design being a biomimetic arrangement of the natural palmitoylation phenomena shown in figure 4-1. Because of this, these studies would present advancing results favoring further understanding of the proteolytic interactions involving BoNTA/LC proteases and SNARE substrates.

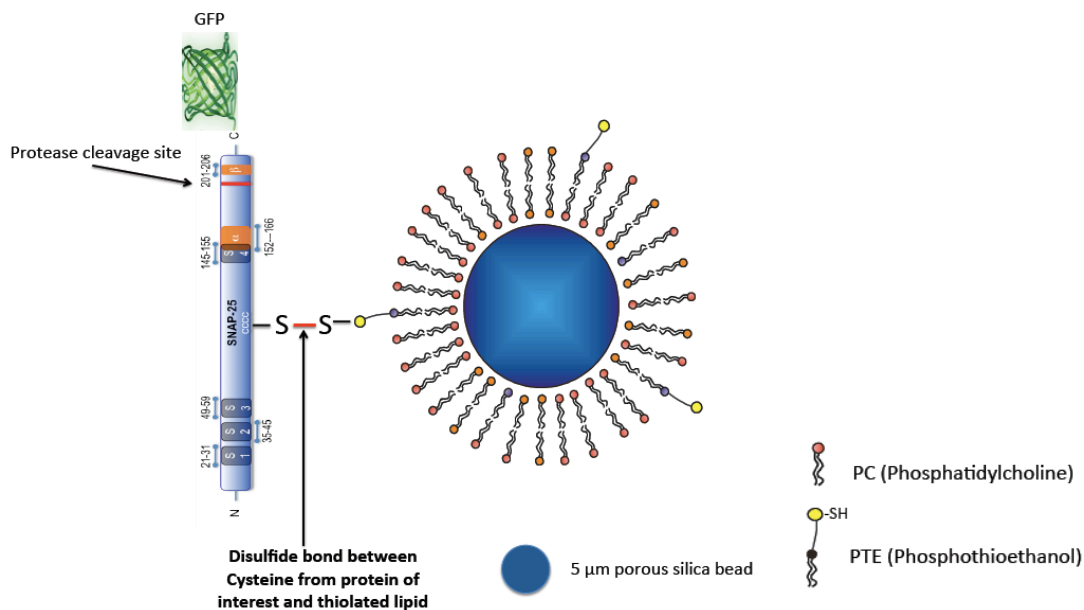


**Figure 4-2.** Disulfide bond formation between cysteine residues from SNAP-25 and thiolated SLBs. Silica beads covered by supported lipid bilayers are formed by spontaneous vesicle fusion. One can form lipid platforms of one or more types of lipids depending on the application of interest. Here, phosphatidylcholine lipids are mixed with smaller molar fractions of phosphothioethanol lipid in order to form disulfide bridges with cysteine residues from SNAP-25.

## 4.2 Materials and Methods

### 4.2.1 Surface Treatment of Silica Microspheres

Mesoporous silica beads with 5 nm in pore size and 5 μm in diameter were obtained from Macherey-Nagel (Duren, Germany). In order to obtain clean, hydrophilic bead surfaces, treatment processes were applied as previously described.<sup>13</sup> Briefly, beads were washed with ethanol and then DI water several times, respectively. Then they were suspended in a 40 mL solution containing freshly mixed 4% H<sub>2</sub>O<sub>2</sub> and 4% NH<sub>4</sub>OH and placed in an 80° C water bath for 10 min. After several DI water rinses, this was followed by a second treatment in 40 mL freshly made solution of H<sub>2</sub>O<sub>2</sub> and 0.4 M HCl in the 80 °C water bath for 10 min. After additional DI water rinses, the beads were resuspended in

20 mL Tris buffer (100 mM Tris, 150 mM NaCl, pH 7.4). A Coulter Counter was then used to calculate the number of beads per volume.

#### **4.2.2 Preparation of Supported Lipid Bilayers**

All lipids were purchased from Avanti Polar Lipids (Alabaster, AL). Small unilamellar vesicles were prepared from 1mM solutions of either egg phosphatidylcholine (egg PC) or 1-palmitoyl-2-oleoyl-sn-glycero-3-phosphocholine (POPC) in chloroform, in clean glass vials. In addition, 1,2-dihexadecanoyl-sn-glycero-3-phosphothioethanol (PTE), and 1,2-dioleoyl-sn-glycero-3-phosphoethanolamine-N-[3-(2-pyridyldithio)propionate] (PDP-PE), were also used in specific experiments, as described below. A variety of lipid concentrations were used including 1 mol %, 2 mol %, 5 mol %, and 10 mol % of PTE or PDP-PE mixed with the remaining egg PC or POPC lipid. Hamilton syringes were used for lipid and chloroform handling and mixing at all times.

Lipid solutions were then dried under a N<sub>2</sub> stream in order to remove the chloroform and subsequently resuspended in Tris buffer and mixed for 1hr. The samples were then sonicated on water bath for 30 min and then transported to microfuge tubes to be mixed with the surface-treated silica beads. The mixtures were vortexed vigorously for 5 min and then shaken for 25 min at 37 C°. This process allowed the lipid vesicles to spontaneously form supported lipid bilayers surrounding the beads. Finally, the beads were washed several times in Tris buffer to eliminate unbound lipids.

### 4.2.3 Lipid Stability Analysis

Lipid bilayer stability is a crucial characteristic needed for the success of our studies, therefore we tested the SLB stability on beads by using Triton detergent as a lipid bilayer-disrupting agent.<sup>14</sup> First, we loaded the surface-treated porous silica beads with 10 mM fluorescein in Tris buffer by constant vortexing for at least 24 hours. After three washing steps, the beads were coated by lipids at different molar fractions just as described in section 4.2.2. Fluorescein content was then measured in two different ways. We monitored fluorescein content entrapped by the SLBs as well as the amount of fluorescein that leaked towards the aqueous environment outside the membranes. Ideally, we expected to observe minimum fluorescein leakage for several days until a disrupting agent was introduced to the system (e.g. Triton X100 surfactant). We monitored direct fluorescein leakage from the beads using flow cytometry while increase of fluorescein in solution was measured using spectrofluorimetry. Upon bilayer formation we recorded fluorescence intensities using both methods every 5 washing steps for a total of 15 washing steps. Stability measurements were recorded following the 15<sup>th</sup> final wash every 8 hours for several days. In between measurements, the samples were stored at 5°C. Finally, the non-ionic surfactant Triton X100 was added to the samples and mixed for 30 minutes. Fluorescence measurements were once again recorded in order to monitor fluorescein leakage due to SLB disruption.

#### **4.2.4 Biomolecular Assembly and Protease Assays for Flow Cytometry**

SNAP-25 solutions were prepared at different concentrations (100 nM to 500 nM) in Tris buffer. Then, approximately  $6.4 \times 10^6$  prepared SLB-beads consisting of different thiol-lipid concentrations ranging from 0 to 10% were added to microfuge tubes, making a total volume of 500  $\mu$ L in each tube. The Protein-SLB-beads samples were incubated in the dark at different times (1 hour to overnight) in order to monitor time-dependent binding interactions. The samples were analyzed using an Accuri C6 flow cytometer (Becton-Dickinson, San Jose, CA) and further data analysis was performed using flow cytometry analysis software such as FlowJo (Tree Star, Ashland, OR) and FCS Express (De Novo Software, Los Angeles, CA). In order to verify disulfide bridge formation and specific binding, control experiments consisted in the addition of reducing agents such as dithiothreitol (DTT) and 2-mercaptoethanol (BME) to the samples, which lead to fluorescence decrease at the surface of the beads.

BoNTA/LC protease was added to the samples at concentrations ranging from 10 nM to 30 nM, allowing an incubation time of 30 minutes before flow cytometry analysis.

### **4.3 Results**

#### **4.3.1 Lipid Stability Analysis**

Three different PTE concentrations mixed with POPC were used to form SLBs in fluorescein-coated beads for lipid stability studies: 0%, 1%, 2% and 10%. After 15 washing steps following bilayer formation we monitored fluorescence from the beads for 3 days. Minimum fluorescein leakage was observed over this period of time. SLBs

proved to be able to sequester the majority of the fluorescein molecules surrounding the beads, thus verifying lipid bilayer stability over time as reported in the literature. As the concentration of PTE increased, the amount of fluorescein molecules diffusing out of the SLB-bead complex was higher (see figure 4-3). However, SLBs at all PTE concentrations are shown to be much more effective at sequestering fluorescein at the surfaces of the beads than in the case where beads were coated with fluorescein in the absence of SLBs. Upon reaching the 3-day monitoring final point, we added Triton X100 to the beads in solution and after 30 minutes of mixing we were able to observe a drastic fluorescence decrease in all samples. This allowed us to confirm that when a surfactant is present, lipid bilayers no longer possess their stability property, thus promoting fluorescein leakage from the surface of the microspheres. As presented in figure 4-3, fluorescence levels from disrupted SLB-beads were much lower than fluorescein-coated beads without any lipids. This can be explained, in part, by the result of interactions between a non-ionic surfactant such as Triton X100 and an organic fluorescent dyes such as fluorescein, causing a shift to the left in the fluorescein's emission wavelength maxima.<sup>15</sup>

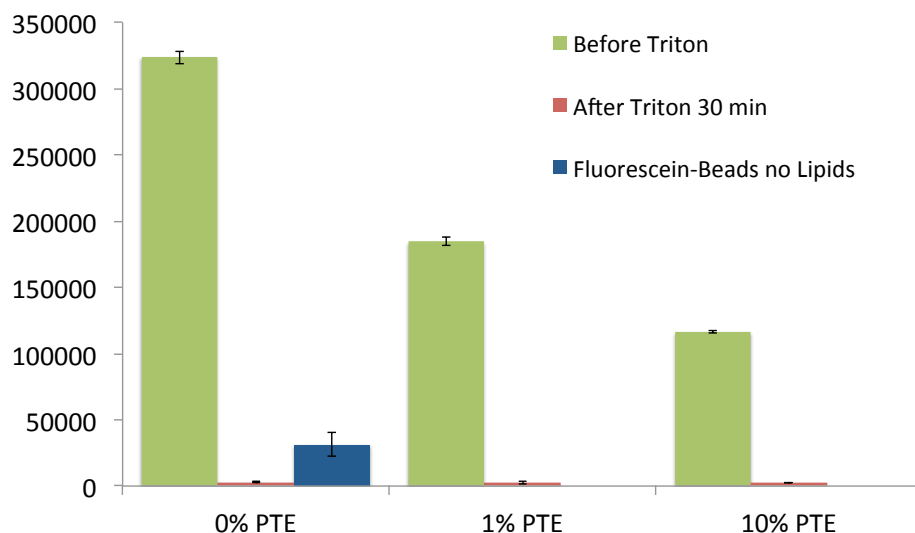


**Figure 4-3.** Fluorescein-Lipid stability tests using flow cytometry. Binary lipid mixtures of POPC and PTE at 100%/0%, 99%/1%, and 90%/10% were used respectively. Porous silica beads were loaded with fluorescein and retained to the bead surface thanks to the formed lipid bilayers and their stability. After achieving a stable fluorescence reading from all samples after 3 days of SLB formation (green), we added SLB disrupting surfactant Triton X100 to each sample and recorded fluorescence change (red). Upon membrane disruption due to the presence of the surfactant, fluorescein is released triggering a significant loss of fluorescence. In addition, we compared these measurements to fluorescein loaded to beads in the absence of SLBs (blue). Fluorescence retention from 90%/10% thiol-SLB mixture was less than half as efficient than the SLB made out of 100% POPC.

### 4.3.2 Biomolecular Assembly and Protease Assays for Flow Cytometry

PTE lipids at varying concentrations of 0%, 1%, 2%, and 10% were used for this part of our studies. The case involving 100% POPC or egg PC was used as a control in order to address nonspecific binding issues. We looked for binding events other than the described disulfide formation by mixing non-thiolated SLBs (100% PC, 0% PTE) with SNAP-25 GFP. According to previous reports on the structural differences between egg PC and POPC<sup>16</sup>, egg PC due to its extraction from natural sources, it contains a higher amount of unsaturated phospholipids than the synthetic POPC<sup>17</sup>. Therefore, POPC will form more ordered and more stable SLBs<sup>16</sup>. This is why we opted to conduct our SLB experiments with POPC.

Flow cytometry analysis provided information on fluorescence signals from three different scenarios: 1) SLBs formed by varying lipid mixtures on microspheres in the absence of SNAP-25 GFP or any fluorescence marker 2) SNAP-25 GFP added to SLBs on beads after different mixing times, and 3) BoNTA/LC protease addition to the previous scenario after 30 minutes of incubation. The first scenario served as a fluorescence background indicator, i.e. GFP is absent in the mixture. The second scenario presented a fluorescence increase by approximately 2 decades compared to the initial scenario when 1%, 2%, and 10% PTE were used. Subsequently, the third scenario presented a fluorescence decrease by 50% to 60% compared to the second scenario. However, the control which contained 0% PTE also presented a significant increase in fluorescence when mixed with SNAP-25 GFP. Featured flow cytometry data in figure 4-4 and 4-5 compare SNAP-25 GFP binding to thiol-SLB structures and SLBs from purely POPC after two hours of incubation as well as 7 days after bilayer formation. In these experiments we intended to prove the binding specificity SNAP-25 to thiols-rich structures. While SNAP-25 GFP possessed the same molecular availability for it to bind to both SLB structures, fluorescence signals from beads bearing thiol-SLBs presented a significant increase over its POPC SLBs counterpart ( $1.25 \times 10^6$  compared to  $2.34 \times 10^5$ ).

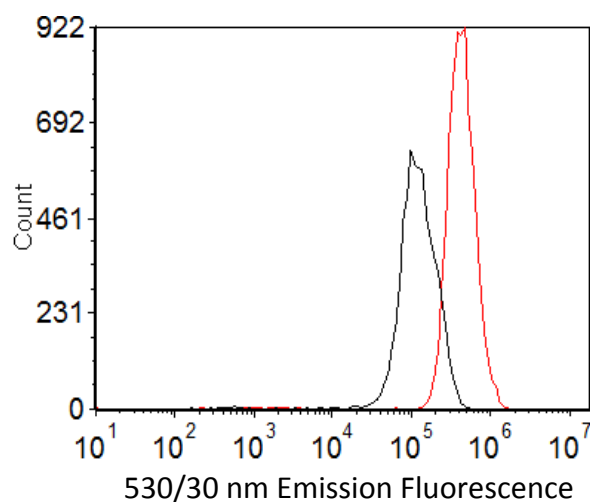


**Figure 4-4.** Flow cytometry test for specificity of SNAP-25 attachment to thiolated SLBs. Samples were incubated for 2 hours before analysis. Black: 100% POPC mixed with 800 nM SNAP-25 GFP. Red: 98% POPC and 2% PTE mixed with 800 nM SNAP-25 GFP. Fluorescence intensity readings from thiol-containing SLB-beads presented 70% higher fluorescence intensity than SLBs composed of POPC only (no thiol-lipids).

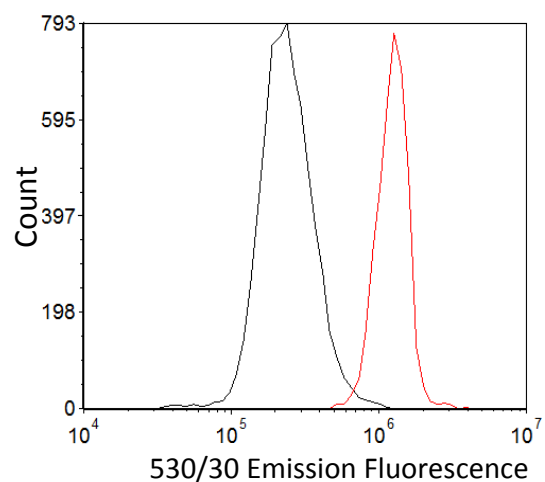


**Figure 4-5** SNAP-25 GFP binding test comparison after 7 days of SLB formation. Black: SLBs containing 100% POPC. Red: 98% POPC and 2% PTE. Fluorescence intensity from the experimental group (red) reached  $1.25 \times 10^6$  fluorescence units, while fluorescence intensity from the control group (black) was of  $2.34 \times 10^5$  fluorescence units, which is 80% less than that of the experimental group.

In order to quantify non-specific interactions originated by the binding of SNAP-25 with POPC lipid membranes, we utilized DTT to act as a selective reducing agent targeting the disulfide bridges formed by SNAP-25 GFP and thiol-rich SLB-beads. Therefore, this compound triggered fluorescence loss at the surface of the beads due to the detachment of SNAP-25 from the complex. The amount of fluorescence signal lost because of the presence of DTT was considered to be associated to specific interactions.

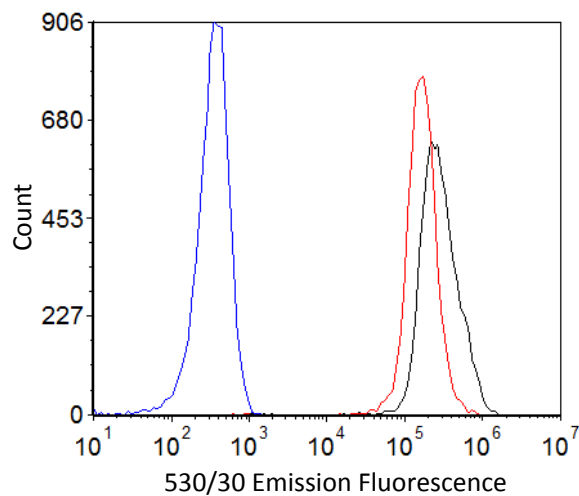


**Figure 4-6.** Reduction of 100% POPC SLBs using DTT. Blue: 100% POPC SLBs on beads without SNAP-25 GFP. Black: 800 nM SNAP-25 GFP bound to 100% POPC SLB beads. Red: Effect of 100 mM DTT after 30 min. mixing with SNAP-25 bearing SLB-beads.

After conducting several experiments involving DTT at varying concentrations, we observed that the addition of 100 mM DTT to the beads caused a fluorescence intensity decrease of 30% to 40%, indicating a considerable amount of non-specific adsorption. DTT incubation time with SNAP-25-bound beads was 2. Finally, we report a BoNTA/LC protease activity assay using thiol-SLBs on beads (figure 4-8) in which the protease shows a certain degree of activity by observing a 58% fluorescence decrease due to presumed cleavage.

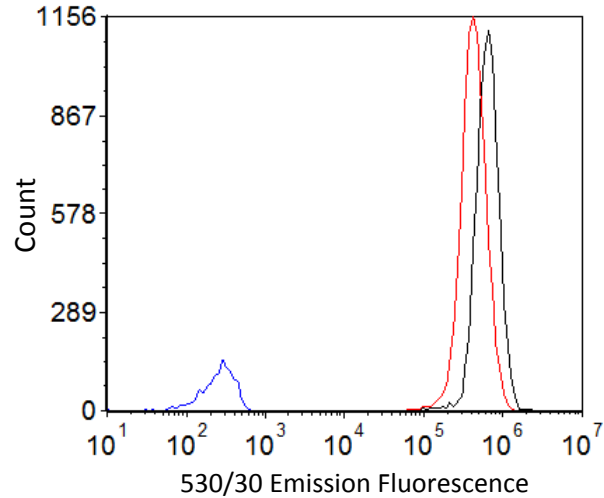


**Figure 4-7.** Reduction of 98% POPC and 2% PTE SLBs on beads using DTT. Blue: 98% POPC and 2% PTE SLBs on beads without SNAP-25 GFP. Black: 800 nM SNAP-25 GFP bound to thiolated SLBs on beads. Red: Effect of 100 mM DTT after 30 min. mixing with SNAP-25 bearing thiol-SLB-beads.

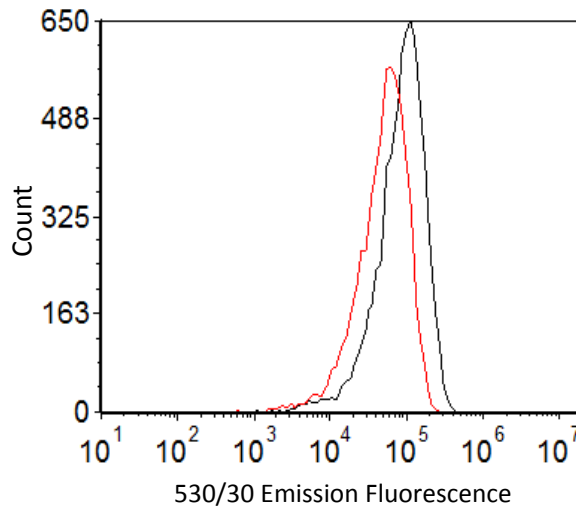


**Figure 4-8.** BoNTA/LC protease assay on PTE/POPC SLBs on beads. Black SNAP-25 GFP binding to 99% POPC/1% PTE SLBs on beads. Red: BoNTA/LC protease mixed with substrate sample in solution for 30 min. prior to flow cytometry analysis. Fluorescence intensity decreased by 58% after apparent cleavage of SNAP-25 GFP substrate.

## **4.4 Discussion and Conclusions**

### **4.4.1 Supported Lipid Stability**

We have successfully developed stable and functional supported lipid bilayers on porous silica microspheres containing binary lipid mixtures selected to promote specific interactions with our proteins of involved in our studies. Lipid bilayer stability tests indicate SLBs on beads are the most stable when prepared with 100% POPC. Based on fluorescein-based stability tests, as the concentration of PTE (thiol-lipid) increased in the bilayer structure, the more fluorescein was allowed to exit the lipid membrane, therefore presenting a less stable SLB structure. Because of these findings, we opted to include lipid mixtures containing up to 2% PTE in our protease assay studies.

### **4.4.2 Biomimetic Platforms for Protease Activity Assays**

We have developed a biomimetic platform designed to resemble the synaptic vesicle docking to the SNARE protein SNAP-25. SLBs consisted of a small fraction of thiol-lipids and a larger one of POPC lipids. PTE concentrations were determined by SLB stability studies, from which we concluded that optimal PTE concentrations were at 1% to 2%. SNAP-25 GFP was added to this lipid-bead arrangement at different concentrations. Our flow cytometry studies allow us to conclude that higher fluorescence readings are found when using SLBs made from these PTE concentrations in comparison to SLBs containing 100% POPC. However, from our flow cytometry information, show significant amount of fluorescence on beads bearing the 100% POPC composition, which indicates the existence of non-specific binding issues. Therefore, quantified this parameter by adding reducing agents BME or DTT in order to reduce the SNAP-25

molecules docked to the thiol-functionalized lipid membranes. Fluorescence intensity readings from beads after this procedure was considered to be corresponding to SNAP-25 molecules bound to the membranes non-specifically. After applying this method in the majority of our experiments, fluorescence intensities were reduced by half. This constraint can be attributed to the hydrophobic regions present in our substrate protein complex, which is composed of a biotinylation region of approximately 100 amino acids residues, the SNAP-25 sequence region, and the GFP region. Therefore, this synthetic component is greater in size than the wild type SNAP-25, which creates a higher chance for steric hindrance once in contact with the SLB on microspheres.

## References

1. Sollner, T.; Bennett, M. K.; Whiteheart, S. W.; Scheller, R. H.; Rothman, J. E., A PROTEIN ASSEMBLY-DISASSEMBLY PATHWAY IN-VITRO THAT MAY CORRESPOND TO SEQUENTIAL STEPS OF SYNAPTIC VESICLE DOCKING, ACTIVATION, AND FUSION. *Cell* **1993**, 75 (3), 409-418.
2. Gonzalo, S.; Linder, M. E., SNAP-25 palmitoylation and plasma membrane targeting require a functional secretory pathway. *Molecular Biology of the Cell* **1998**, 9 (3), 585-597.
3. Veit, M.; Sollner, T. H.; Rothman, J. E., Multiple palmitoylation of synaptotagmin and the t-SNARE SNAP-25. *Febs Letters* **1996**, 385 (1-2), 119-123.
4. Rothman, J. E., MECHANISM OF INTRACELLULAR PROTEIN-TRANSPORT. *Nature* **1994**, 372 (6501), 55-63.
5. Veit, M., Palmitoylation of the 25-kDa synaptosomal protein (SNAP-25) in vitro occurs in the absence of an enzyme, but is stimulated by binding to syntaxin. *Biochemical Journal* **2000**, 345, 145-151.
6. Greaves, J.; Prescott, G. R.; Fukata, Y.; Fukata, M.; Salaun, C.; Chamberlain, L. H., The Hydrophobic Cysteine-rich Domain of SNAP25 Couples with Downstream Residues to Mediate Membrane Interactions and Recognition by DHHC Palmitoyl Transferases. *Molecular Biology of the Cell* **2009**, 20 (6), 1845-1854.
7. Daily, N. J.; Boswell, K. L.; James, D. J.; Martin, T. F. J., Novel Interactions of CAPS (Ca<sup>2+</sup>-dependent Activator Protein for Secretion) with the Three Neuronal SNARE Proteins Required for Vesicle Fusion. *Journal of Biological Chemistry* **2010**, 285 (46), 35320-35329.
8. Koticha, D. K.; McCarthy, E. E.; Baldini, G., Plasma membrane targeting of SNAP-25 increases its local concentration and is necessary for SNARE complex formation and regulated exocytosis. *Journal of Cell Science* **2002**, 115 (16), 3341-3351.
9. Chen, S.; Hall, C.; Barbieri, J. T., Substrate recognition of VAMP-2 by botulinum neurotoxin B and tetanus neurotoxin. *Journal of Biological Chemistry* **2008**, 283 (30), 21153-21159.
10. Bayerl, T. M.; Bloom, M., PHYSICAL-PROPERTIES OF SINGLE PHOSPHOLIPID-BILAYERS ADSORBED TO MICRO GLASS-BEADS - A NEW VESICULAR MODEL SYSTEM STUDIED BY H-2-NUCLEAR MAGNETIC-RESONANCE. *Biophysical Journal* **1990**, 58 (2), 357-362.
11. Chemburu, S.; Fenton, K.; Lopez, G. P.; Zeineldin, R., Biomimetic Silica Microspheres in Biosensing. *Molecules* **2010**, 15 (3), 1932-1957.

12. Hess, D. T.; Slater, T. M.; Wilson, M. C.; Skene, J. H. P., THE 25 KDA SYNAPTOSOMAL-ASSOCIATED PROTEIN SNAP-25 IS THE MAJOR METHIONINE-RICH POLYPEPTIDE IN RAPID AXONAL-TRANSPORT AND A MAJOR SUBSTRATE FOR PALMITOYLATION IN ADULT CNS. *Journal of Neuroscience* **1992**, *12* (12), 4634-4641.
13. Buranda, T.; Huang, J.; Ramarao, G. V.; Ista, L. K.; Larson, R. S.; Ward, T. L.; Sklar, L. A.; Lopez, G. P., Biomimetic molecular assemblies on glass and mesoporous silica microbeads for biotechnology. *Langmuir* **2003**, *19* (5), 1654-1663.
14. Zeineldin, R.; Piyasena, M. E.; Bergstedt, T. S.; Sklar, L. A.; Whitten, D.; Lopez, G. P., Superquenching as a detector for microsphere-based flow cytometric assays. *Cytometry Part A* **2006**, *69A* (5), 335-341.
15. Mathur, A. K.; Agarwal, C.; Pangtey, B. S.; Singh, A.; Gupta, B. N., SURFACTANT-INDUCED FLUORESCENCE CHANGES IN FLUORESCCEIN DYE. *International Journal of Cosmetic Science* **1988**, *10* (5), 213-218.
16. Rye, K. A.; Hime, N. J.; Barter, P. J., The influence of sphingomyelin on the structure and function of reconstituted high density lipoproteins. *Journal of Biological Chemistry* **1996**, *271* (8), 4243-4250.
17. Kuksis, A., YOLK LIPIDS. *Biochimica Et Biophysica Acta* **1992**, *1124* (3), 205-222.

## **Chapter 5**

### **Conclusions and Recommendations for Future Work**

#### **5.1 Surface-based Protease Assays for Surface Plasmon Resonance Analysis**

##### **5.1.1 Conclusions**

In chapter 2 we have demonstrated the binding capabilities of SAMs on gold substrates for protein immobilization. We have successfully fabricated SPR sensor chips functionalized with biotinylated thiols for streptavidin immobilization. This approach provides a simple path for assessment of a variety of bioassays. The nature of the streptavidin/biotin interaction high binding constant ( $K_a \approx 10^{13} \text{ M}^{-1}$ )<sup>1</sup> has proven to be a robust tool for its capabilities of forming strong molecular building blocks, and for the study of protein-surface interactions.

We have gained a significant amount of knowledge in microbiological techniques associated with the process of expression and purification of proteins. Consequently, as part of the methodology involved for the completion of our studies, we have successfully expressed and purified the SNAP-25 protein coupled with a biotinylation region and a GFP region on opposite ends of the protein for streptavidin-binding and fluorescence recognition, respectively. While SPR allows for label-free detection, we utilized the additional amino acid sequence in our design in order to maximize the amount of mass that could be potentially cleaved by proteases of interest, and thus reducing ambiguous data. Biomolecular assembly of streptavidin and SNAP-25 GFP onto the surface of our fabricated SPR sensor chips has been presented in binding assays. As expected, binding of streptavidin to the biotin-rich sensor surface has been demonstrated via SPR by

observing increase of resonance signal due to injected streptavidin binding to the surface. Subsequent injection of biotinylated SNAP-25 showed further increase the resonance signal. Such response signals have been quantified by accounting for the change in response units given by the instrument upon binding.

After several trials involving proteases introduced to the SPR instrument and placed in contact with the active sensor surface, resulting signals deviate from our predicted protease response. While the proteases present binding response signals once in contact with the exposed substrates, no significant cleavage can be appreciated. This can be explained by the hindering effect from GFP molecules, preventing efficient contact between the protease and the substrate. For the case involving BoNTA/LC protease detection, injected protease association response signals nearly equaled the dissociation signals, which indicated nonspecific binding to the SNAP-25 GFP substrate complex. The case involving lethal factor protease detection (figure 2-9) suggests specific binding response signals in all biological components. Cleavage response is very slow, nonetheless this is in good agreement with the bead-based protease assays reaction times reported elsewhere<sup>2</sup>.

Finally, we conclude that several parameters have be taken into consideration for their contributions to hinder effective protease assays. These are: SAM organization and molecular ordering, impurities from recombinant protein extraction procedures, protein denaturation effects, geometry of sensor surfaces (flat, rectangular surface area as opposed to previous reports on spherical surfaces), and non-specific binding. We have demonstrated that SPR-based analytical techniques are valuable for protease kinetics by providing with real time methods to recognize and segregate the time corresponding substrate-binding events from that of the proteolytic/cleavage events.

### 5.1.2 Recommendations for Future Work

One of the disadvantages from this adopted technique is the reproducibility issue concerning SPR binding responses. Initial baselines varied significantly, which denotes varying SAM content at the sensor chips. This triggered different SPR response signals when proteins of interest were introduced to the system. Previously reported studies<sup>3</sup> indicate that SAMs formed by biotinylated thiols are disordered and their headgroups do not show specific orientation, thus making streptavidin immobilization less efficient by contributing to non-specific interactions. A proposed solution for more order biotinylated SAMs has also been published<sup>3</sup> and it consists of SAMs formed by binary thiol mixtures incorporating a second shorter hydrophobic thiol. This arrangement promotes closely packed, more organized SAMs. Determining optimal molar fractions of the thiols in question require further analysis and more complexity. Using X-ray photoelectron spectroscopy (XPS) allows one to build a correlation between the surface composition of the SAM and the mole fractions in solution<sup>4</sup>.

An additional alternative for enhancing surface sensor chip design is the implementation of SAMs terminated with a nitrilotriacetic acid (NTA) group, which is known to form a tetravalent chelate with Ni (II)<sup>5</sup>. This approach is to be coupled with proteins of interest that contain a termination of commonly six histidines in their sequence. Therefore, recombinant his-tagged SNAP-25 GFP and LF-15 substrates could specifically bind to SPR sensor chips rich in NTA-SAMs, reducing the longer peptide sequence presented in this work (biotinylation sequence), thus minimizing the amount of non-specific adsorption.

## **5.2 Packed-bed Microfluidic Devices for Protease Analysis**

### **5.2.1 Conclusions**

The Packed-bed microfluidic channel approach is a biosensing technique that can be adopted for a variety of bioanalytical assays. Our devices presented ease in portability and great efficiency at sample and buffer consumption. They were inexpensive to fabricate and allowed us to design multiple channels on one chip for the analysis of different compounds and controls. We have demonstrated, as presented in figure 3-4 and figure 3-7, simple qualitative and quantitative methods for protease detection via fluorescence microscopy and fluorimetry, respectively. However, we encountered several constraints that need to be addressed in order to improve the protease assay process development. 1) There is a dominance of mass transport over kinetics, which is reaffirmed by backpressure build up in the channels due to expansion of the PDMS microfluidic walls. 2) The devices presented reproducibility issues due to the nature of their fabrication process. While we reduced the cost of the micro-fabrication process, we were limited to roughly 10  $\mu\text{m}$  in channel width and height. This constraint makes them unsuitable for the packing of microspheres of less than 10  $\mu\text{m}$  in diameter because they would flow through the dam, towards the channel outlet.

## 5.2.2 Recommendations for Future Work

In order to build microfluidic devices at smaller dimensions, capable of analyzing smaller beads we suggest the implementation of deep reactive-ion etching (DRIE) to the fabrication process. This cleanroom technique allows for the development of microchannel sizes lower than 10  $\mu\text{m}$  and greater fidelity than our described softlithographic techniques. This improved approach will reduce channel backpressure by substituting PDMS for a better precursor material capable of eliminating expansion effects at the channel's walls. Hence, microfluidic channel characterization would be enhanced for the analysis of mass transfer and reaction kinetics parameters<sup>6</sup>.

We have presented assays based on the loss of fluorescence at the surface of streptavidin polystyrene beads. Because of this, we have started at a given GFP fluorescence level indicated by the substrate and finished at reduced fluorescence intensities due to the cleavage effect by the protease. In addition, further consistency in fluorescence measurements can be achieved by developing assays based on gain in fluorescence rather than loss of fluorescence. This can be done by exploring fluorescence resonance energy transfer (FRET) approaches<sup>7, 8</sup>. An example of FRET pairs that are suitable and recommended for these studies include Pacific Blue (exc.  $\sim 410$  nm, em.  $\sim 455$  nm) or Alexa 405 (exc.  $\sim 402$  nm, em.  $\sim 421$  nm) as the donor component, and GFP (exc.  $\sim 489$  nm, em.  $\sim 509$  nm) as the acceptor component. In this scenario, we would mix a blue dye-labeled streptavidin with SNAP-25 GFP, such that fluorescence is transferred from donor molecules to the acceptor molecules. Thus, donor molecules lose fluorescence while the acceptor SNAP-25 GFP complex gains fluorescence. Once BoNTA/LC cleavage of the SNAP-25 GFP substrate complex occurs, GFP is freed which

in turn, terminates FRET. In this manner, we would be able to monitor gain in fluorescence at the donor's side and as a result, analyze the BoNTA/LC activity.

## **5.3 Biomimetic Platforms for Protease Diagnostics**

### **5.3.1 Conclusions**

We have successfully developed fluidic membranes on microspheres capable of sustaining biological compounds and of carrying reactions at the surface of beads. Phospholipid membrane contents were formed to mimic natural membranes found in neurons whose role is to promote synaptic vesicle fusion (palmitoylation). Specifically, we have studied supported lipid bilayers containing PTE lipids or PDP-PE lipids. The first one consists of thiolated headgroups, and the second one contains pyridyldithiol groups (disulfide). They were both studied in SLBs while mixed with more abundant POPC or Egg PC lipids. We intended to recreate the binding process of palmitoylation between these membranes and recombinant SNARE protein SNAP-25 GFP. We believe that specific binding in the form of disulfide bridges between SNAP-25's cysteine's thiols and thiol-rich SLBs were formed when using molar percentages of 1%, 2% and 5% PDP-PE or PTE. We were able to discriminate between specific and non-specific binding events by utilizing DTT as a membrane disrupting agent in our experiments by reducing these complexes at their disulfide bridges and thus, attributing the rest of membrane-bound protein to non-specific interactions. We believe non-specificity was considerably high due to the additional amino acid residues present in our recombinant protease substrate. 1) Part of this issue is due to the presence of cysteines in GFP's amino acid sequence, which can be seen at [http://www.uniprot.org/blast/?about=P42212\[1-238\]](http://www.uniprot.org/blast/?about=P42212[1-238]). 2)

This issue can also be explained by the presence of possible impurities in SNAP-25 originated by the protein's expression and purification process. 3) Amino terminal biotinylation tags of approximately 100 amino acid residues may also have provided non-specific SNAP-25 binding sites.

Flow cytometric BoNTA/LC protease assays performed using described SLBs have proved to present active substrate cleavage by observing fluorescence reduction of 60% on SNAP-25 GFP-bearing microspheres. These results are promising and provide room for improvement, which include appropriate and timely handling of all proteases and substrate proteins, and reduction of non-specific binding between protease substrates and membranes. Flow cytometry has proven to be a time-efficient, simple to operate, and overall, a more robust technique for our desired protease assays than techniques described in previous chapters.

### **5.3.2 Recommendations for Future Work**

Given the advantages that flow cytometry provides to our protease assay development process, one will be able to conduct protease assays involving all SNARE proteins bound to microspheres simultaneously. Furthermore, as stated previously, there are ongoing research efforts in the area of high throughput screening and protease activity detection of all BoNT protease types involved in disease<sup>9, 10, 11</sup>. Our methods and findings provide meaningful contributions to these areas and at a greater degree if we improve the design of biomimetic surfaces capable binding with SNAP-25 in a specific manner. High throughput screening and multiplexing efforts currently feature static biomolecular conjugations and interactions. Our studies would enhance these areas of studies thanks to the fluidity and stability presented by SLBs.

In addition, we propose the application of histidines/Ni-NTA complex formation approaches in our flow cytometry studies. Vector plasmids for recombinant His-tagged proteins can be easily obtained from a variety of commercial sources. Coupling studies of His-tagged proteins to biomimetic membranes is a subject of ongoing research in our laboratory.

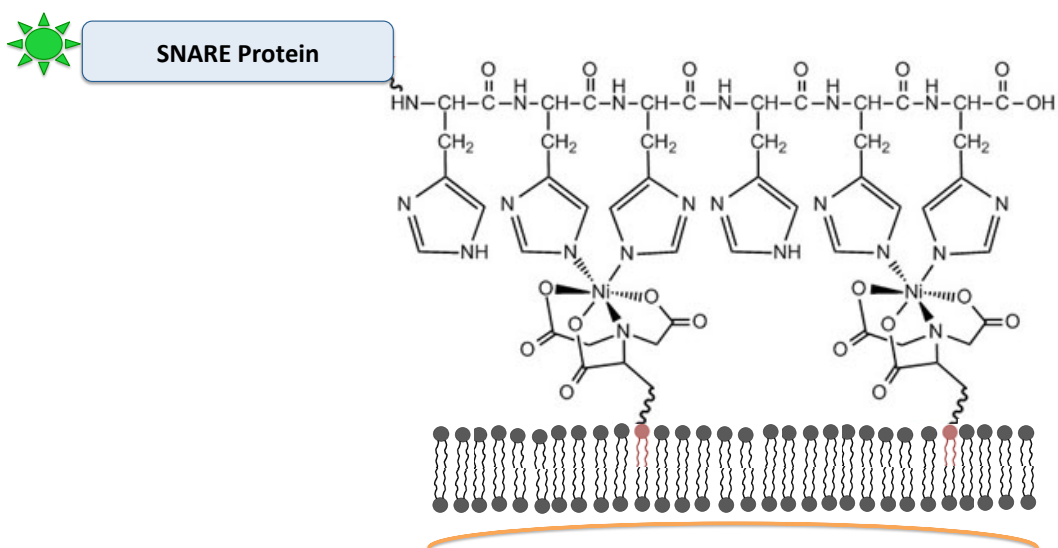


**Figure 5-1.** Recombinant SNARE protein with six terminal histidines binds to Ni-NTA functionalized SLBs on microspheres. These proteins can be easily purified by known chromatography techniques, yielding His-tagged and GFP-tagged proteins with high efficiency.

## References

1. Green, N. M., Avidin. *Advances in Protein Chemistry* **1975**, *29* (1), 85-133.
2. Saunders, M. Microsphere based protease assays and high throughput screening of bacterial toxin proteases. Dissertation, University of New Mexico, 2010.
3. Perez-Luna, V. H.; O'Brien, M. J.; Opperman, K. A.; Hampton, P. D.; Lopez, G. P.; Klumb, L. A.; Stayton, P. S., Molecular recognition between genetically engineered streptavidin and surface-bound biotin. *Journal of the American Chemical Society* **1999**, *121* (27), 6469-6478.
4. Nelson, K. E.; Gamble, L.; Jung, L. S.; Boeckl, M. S.; Naeemi, E.; Golledge, S. L.; Sasaki, T.; Castner, D. G.; Campbell, C. T.; Stayton, P. S., Surface characterization of mixed self-assembled monolayers designed for streptavidin immobilization. *Langmuir* **2001**, *17* (9), 2807-2816.
5. Sigal, G. B.; Bamdad, C.; Barberis, A.; Strominger, J.; Whitesides, G. M., A self-assembled monolayer for the binding and study of histidine tagged proteins by surface plasmon resonance. *Analytical Chemistry* **1996**, *68* (3), 490-497.
6. Losey, M. W.; Schmidt, M. A.; Jensen, K. F., Microfabricated multiphase packed-bed reactors: Characterization of mass transfer and reactions. *Industrial & Engineering Chemistry Research* **2001**, *40* (12), 2555-2562.
7. Nichols, J. W.; Pagano, R. E., RESONANCE ENERGY-TRANSFER ASSAY OF PROTEIN-MEDIATED LIPID TRANSFER BETWEEN VESICLES. *Journal of Biological Chemistry* **1983**, *258* (9), 5368-5371.
8. Dong, M.; Tepp, W. H.; Johnson, E. A.; Chapman, E. R., Using fluorescent sensors to detect botulinum neurotoxin activity in vitro and in living cells. *Proceedings of the National Academy of Sciences of the United States of America* **2004**, *101* (41), 14701-14706.
9. Saunders, M. J.; Graves, S. W.; Sklar, L. A.; Oprea, T. I.; Edwards, B. S., High-Throughput Multiplex Flow Cytometry Screening for Botulinum Neurotoxin Type A Light Chain Protease Inhibitors. *Assay and Drug Development Technologies* **2010**, *8* (1), 37-46.
10. Edwards, B. S.; Zhu, J.; Chen, J.; Carter, M. B.; Thal, D. M.; Tesmer, J. J. G.; Graves, S. W.; Sklar, L. A., Cluster cytometry for high-capacity bioanalysis. *Cytometry Part A* **2012**, *81A* (5), 419-429.
11. Marconi, S.; Ferracci, G.; Berthomieu, M.; Kozaki, S.; Miquelis, R.; Boucraut, J.; Seagar, M.; Leveque, C., A protein chip membrane-capture assay for botulinum neurotoxin activity. *Toxicology and Applied Pharmacology* **2008**, *233* (3), 439-446.

